Sustainable Design and Synthesis of Algae-Based Biorefinery for Simultaneous Hydrocarbon Biofuel Production and Carbon Sequestration

Berhane H. Gebreslassie, Randall Waymire, and Fengqi You
Dept. of Chemical and Biological Engineering, Northwestern University, Evanston, IL 60208

DOI 10.1002/aic.14075
Published online March 16, 2013 in Wiley Online Library (wileyonlinelibrary.com)

The superstructure optimization of algae-based hydrocarbon biorefinery with sequestration of CO_2 from power plant flue gas is proposed. The major processing steps include carbon capture, algae growth, dewatering, lipid extraction and power generation, and algal biorefinery. We propose a multiobjective mixed-integer nonlinear programming (MINLP) model that simultaneously maximizes the net present value (NPV) and minimizes the global warming potential (GWP) subject to technology selection constraints, mass balance constraints, energy balance constraints, technoeconomic analysis constraints, and environmental impact constraints. The model simultaneously determines the optimal decisions that include production capacity, size of each processing unit, mass flow rates at each stage of the process, utility consumption, economic, and environmental performances. We propose a two-stage heuristic solution algorithm to solve the nonconvex MINLP model. Finally, the bicriteria optimization problem is solved with ε-constraint method, and the resulting Pareto-optimal curve reveals the trade-off between the economic and environmental criteria. The results show that for maximum NPV, the optimal process design uses direct flue gas, a tubular photobioreactor for algae growth, a filtration dewatering unit, and a hydroprocessing pathway leading to 47.1 MM gallons of green diesel production per year at \$6.33/gal corresponding to GWP of 108.7 kg CO_2-eq per gallon. © 2013 American Institute of Chemical Engineers
AIChE J, 59: 1599–1621, 2013
Keywords: sustainability, biorefinery, mixed-integer nonlinear programming, superstructure, multiobjective

Introduction

In recent years, biomass-derived fuels have received increasing attention as a solution to the nation's continued and growing dependence on imported petroleum-based fuels, which exposes the country to the risk of critical disruptions in fuel supply and concern of climate changes. With this respect, the Energy Independence and Security Act of 2007 (EISA) established a mandatory Renewable Fuel Standard (RFS) requiring transportation fuel sold in the U.S. to contain a minimum of 36 billion gallons of renewable fuels, including advanced and cellulosic biofuels and biomass-based diesel, by 2022. Algal biofuels offer great promise to meet the RFS mandate established within EISA. Potential oil yields from certain algae strains are projected to be at least 60 times higher than that from soybeans, approximately 15 times more productive than jatropha, and approximately five times of that of oil palm per acre of land on an annual basis.[1] Some of the aspects of algal biofuel production that have combined to capture the interest of researchers and entrepreneurs around the world include:

- High productivity of biomass yields per acre of cultivation.
- Use of otherwise nonproductive, nonarable land, and avoids nutrients used for conventional agriculture.
- Nonfood-based feedstock resources.
- Reduced competition for limited freshwater supplies by utilizing waste water, produced water, and saline water.
- Potential recycling of carbon from CO_2-rich flue gas emissions from stationary sources, including power plants and other industrial emitters.

Currently, the term carbon capture and sequestration (CCS) is about the geological storage of CO_2 and in the oil and gas industry the injection of CO_2 into reservoirs is mainly for increasing the yield of fossil hydrocarbon reserves, instead of long-term storage. The biggest difficulties with these approaches are the added cost and power consumption of separation of the CO_2 from both the emission streams and transportation. Algae can also use flue gas or other large sources of carbon dioxide in their growth and the final product is compatible with existing infrastructure for oil and fuel distribution.[1] In this work, we consider algal systems for biological capture of CO_2 to generate useful biomass feedstock for the production of hydrocarbon biofuels. Carbon capture for biofuels reduces the consumption of primary nonrenewable energy resources and the carbon captured by algae is considered as a true sequestration pathway.

Additional Supporting Information may be found in the online version of this article.

Correspondence concerning this article should be addressed to F. You at you@northwestern.edu.

Despite their potential, the state of technology for producing algae-based biofuels is regarded by many in the field to be in its infancy and there is a need of a considerable amount of R&D to achieve affordable, scalable, and sustainable algae-based biofuel production.[1] Hence, the goal of this work is to propose a comprehensive superstructure of sustainable algae-based hydrocarbon biorefinery with the sequestration of carbon dioxide from the flue gas of a power plant. Based on the proposed superstructure, a multiobjective mixed-integer nonlinear programming (MINLP) model is formulated to determine the optimal design and operation of the superstructure under economic and environmental criteria. The processing steps encompass carbon capture from power plant flue gas, gas transportation, algae growth, harvesting, dewatering, drying, lipid extraction, anaerobic digestion, power generation, and algal oil upgrading. A two-stage heuristic solution algorithm is proposed to solve the resulting nonconvex MINLP model. In the first stage, the original problem is reformulated into mixed-integer linear programming (MILP) model by introducing a piecewise linear approximation for the nonlinear terms. The MILP model is solved to obtain a good-quality starting point for the original MINLP problem, which is then solved to simultaneously maximize the net present value (NPV) and minimize the environmental impact measured by global warming potential (GWP) metric that follows the life cycle assessment (LCA) procedure subject to technology selection constraints, design, and operational constraints, which include mass and energy balance constraints, technoeconomic analysis constraints, and life cycle environmental impact constraints. The model simultaneously determines the optimal decisions that include production capacity, size of each processing unit, flow rates of species and streams at each stage of the process, heat, electricity, and natural gas consumption, economic performance, and environmental impacts. The economic objective function takes into account the processing limits, demand of products, selling prices of the main diesel product, and side products such as glycerol and propane. On the other hand, the environmental objective measured by the GWP metric follows the LCA procedures, and considers the cradle-to-gate environmental impact analysis of the algal biorefinery. The solution of the proposed bicriteria MINLP problem produces a Pareto-optimal curve that reveals the trade-off between the environmental concern and economic performance.

Although the optimal design and synthesis of algae-based biorefinery, which integrates superstructure optimization model with technoeconomic analysis and life cycle environmental impact assessment, has not been addressed yet, the literature most relevant to the problem addressed in this work are reviewed below.

There are some existing research works that addressed the optimal design and synthesis of biomass-based energy systems, but they consider economic performance as the only objective function and none of them integrates LCA into the process optimization framework. Chen et al.[2] addressed the optimal design and operation of flexible polygeneration systems using coal and biomass to produce power, liquid fuels, and chemicals. The problem is a multiperiod optimization problem that is nonconvex MINLP. Baliban et al.[3] proposed an MINLP model for the superstructure optimization of thermochemical conversion of combination of coal, natural gas, and biomass to liquid transportation fuels. The MINLP model for the process synthesis includes simultaneous heat and power integration using heat engines to recover electricity from the process waste heat. Martin and Grossmann[4] proposed an MINLP model for the conceptual design of the bioethanol process from switchgrass via gasification. The proposed superstructure considers: direct or indirect gasification, followed by steam reforming or partial oxidation. Membrane separation, absorption, and pressure swing adsorption (PSA) were considered for the removal of sour gases. Two synthetic paths, high alcohols catalytic process and syngas fermentation with distillation, adsorption in corn grits, molecular sieves, and pervaporation as an alternative dehydration processes were considered. The same authors, Grossmann and Martin[5] proposed a mathematical programming techniques to address the optimal energy and water consumption of biofuel process flow sheet that produce bioethanol from corn and switchgrass. Liu et al.[6] proposed a MILP model for optimal design of a polygeneration system that produce concurrently methanol and power using coal, natural gas, and biomass as raw materials. The NPV is maximized by optimizing the combinations of the different feedstocks and the alternative unit operation technologies. The authors expanded the initial optimization model of the polygeneration systems by considering the environmental impact as an additional objective function to be minimized.[7] Wang et al.[8] proposed a multiobjective MINLP model for the superstructure optimization of a hydrocarbon biorefinery via gasification and Fisher–Tropsch synthesis under economic and environmental criteria. The superstructure considers alternative gasification technologies, syngas cooling, hydrogen production technologies, and Fisher–Tropsch synthesis catalysts. Gebreslassie et al.[9] proposed a bicriteria nonlinear programming model for the optimal design and operation of a hydrocarbon biorefinery via fast pyrolysis, hydrotreating, and hydrocracking of hybrid poplar feedstock under economic and environmental criteria. The model is solved by simultaneously maximizing the NPV and minimizing the environmental impacts. The later criterion is measured with GWP metric according to the LCA procedures. Martin and Grossmann[10] addressed the optimal production of second-generation biodiesel via transesterification of waste cooking oil and algal oil feedstocks. They consider five different transesterification technology alternatives. The optimization results indicate that for algal oil, the optimal process employs alkali as the catalyst and at production cost of 0.42 $/gal, and for cooking oil, the optimal process is the one with the heterogeneous catalyst and at production cost of $0.66/gal. West et al.[11] perform four 8000 tonnes/year capacity biodiesel processing technologies simulation using HYSYS to evaluate and compare the economic performance of the technologies. The results indicate that the heterogeneous acid catalyst process was the most economical alternative. Based on process simulation, Gutierrez et al.[12] proposed an integrated production of biodiesel from palm oil using *in situ* produced bioethanol and evaluate the economic viability of the integrated system. Severson et al.[13] proposed a superstructure for the conceptual optimal design of the production of biodiesel using ethanol as the alcohol for the transesterification of algal oil. Davis et al.[14,15] studied baseline economics for two microalgae pathways, by performing a comprehensive analysis using a set of assumptions for what can be reasonably achieved within a 5-year timeframe. On completing the base case scenarios, the cost of lipid production to achieve a 10% return was determined to be $8.52/gal for open ponds (OP)

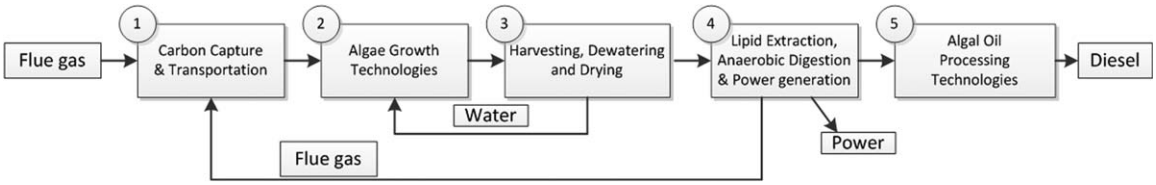

Figure 1. Overview of the major processing steps for carbon capture and sequestration and algae based biofuel production.

and \$18.10/gal for photobioreactors (PBRs). Pokoo-Aikins et al.[16] addressed the design and technoeconomic analysis of an integrated system for the production of biodiesel from algal oil via the sequestration of carbon dioxide from the flue gas of a power plant. A process simulation using ASPEN Plus was carried out to model a two-stage alkali-catalyzed transesterification pathway for the conversion of microalgal oil of Chlorella species to biodiesel.

LCA is the standard procedure to evaluate the environmental performance of a product, process, or activity.[17,18] The first step in the application of LCA includes setting the boundaries for the LCA analysis, defining the objective, the functional unit, and the environmental metrics followed by identification and quantification of the energy and material used in a process. The next step is quantifying the waste released to the environment associated with the energy and material use. This information is further translated into a set of environmental impacts. These impacts are finally used to assess the algal biorefinery design alternatives that may be implemented to achieve a reduction in environmental impact. The large environmental footprint of algae cultivation is driven predominantly by upstream impacts, such as the demand for CO_2 and fertilizer. However, there is lack of literature sources on rigorous optimization strategies of algal biorefinery that consider explicitly the environmental impact as an objective function to be minimized.

The major novelties of this work are summarized as

- The first comprehensive superstructure that considers alternative technologies in the major stages of the synthesis of algal hydrocarbon biorefinery.
- The first comprehensive mathematical programming model for rigorous optimization and synthesis of algal biorefinery for simultaneous production of hydrocarbon biofuels and CCS.
- A life cycle optimization framework for algae-based hydrocarbon biorefinery that integrates the technoeconomic analysis and the environmental impact analysis through a multiobjective optimization framework.
- The Pareto-optimal solutions reveal that the minimum unit production cost of the biofuels ranges from \$6.33 per gallon of diesel and 5121.9 $ktonCO_{2\text{-eq}}$/year GWP for the maximum NPV design, to \$77.7 per gallon of diesel and 3610.6 $ktonCO_{2\text{-eq}}$/year GWP for the minimum GWP design.

The rest of this article is organized as follows. The process description of the superstructure is presented in the next section. The "Life Cycle Optimization" approach is introduced in Section Life Cycle Optimization Framework. A formal problem statement is presented in Section Problem Statement. The detailed model formulation is presented in Section Model Formulation. In Section Solution Algorithm, the bicriteria optimization model is presented and the results of the multiobjective optimization problem are discussed. Finally, concluding remarks are presented in the Section Conclusions.

Process Description

The carbon sequestration and algae-based hydrocarbon biorefinery considered in this work is encapsulated by the following five major processes highlighted in Figure 1.

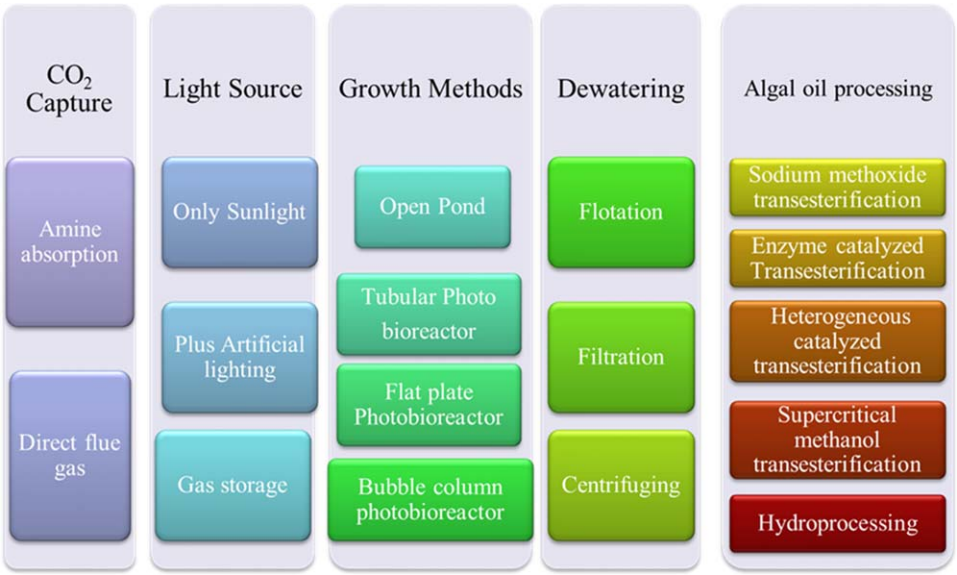

Figure 2. Options considered in the CO_2 sequestration and algae based hydrocarbon biorefinery superstructure.

[Color figure can be viewed in the online issue, which is available at wileyonlinelibrary.com.]

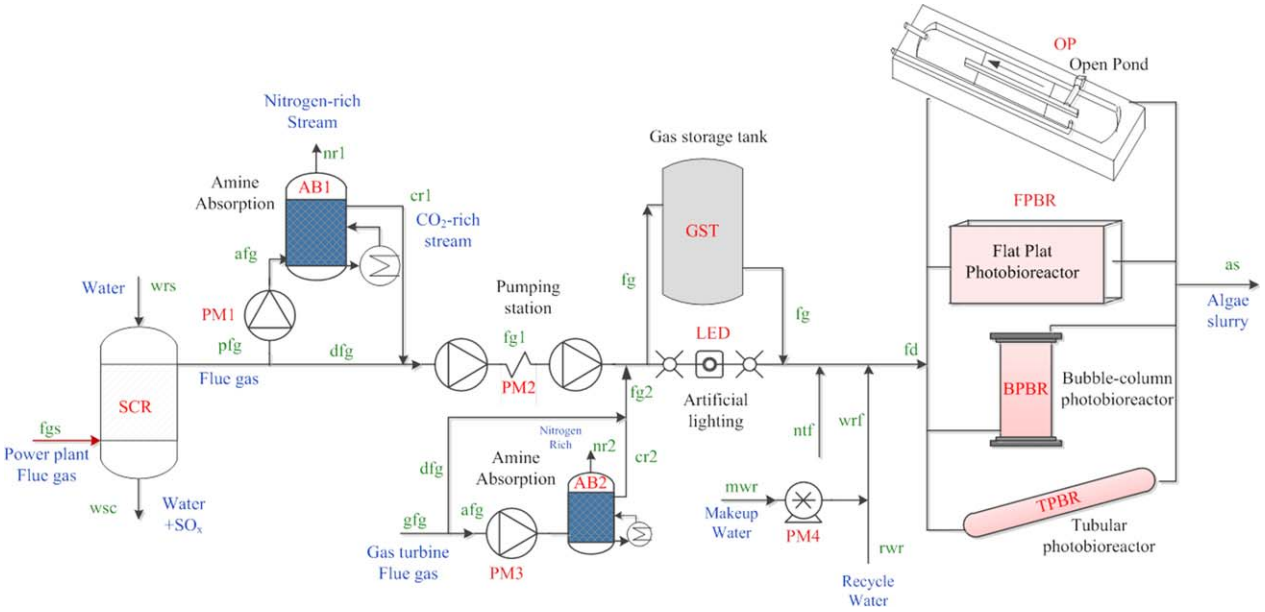

Figure 3. Process flow diagram of carbon capture, CO_2 transportation and algae growth processing sections.

[Color figure can be viewed in the online issue, which is available at wileyonlinelibrary.com.]

In each processing step, there are alternative technologies (Figure 2) that the model must decide based on the economic and environmental performance of the process flow sheet.

Carbon capture and transportation

As shown in Figure 3, the first step in the process is carbon capture. The flue gas that comes off from coal fired power plant is used to nourish the algae that can be used as a feedstock for biofuel production. However, the gas must be collected and processed appropriately for use with algae. The flue gas may be tinged with low concentrations of sulfur in the form of SO_3 and SO_2. Coal fired power plants produce 300–5000 ppm sulfur yet algae cannot survive above a few parts per million. Therefore, a scrubber is used to clean the flue gas. Sulfur interferes with amine absorption if its concentration is above 10 ppm. Therefore, 10 ppm of sulfur is used as a benchmark for the sulfur scrubbing.[19,20] The flue gas from the power plant can be fed to the algae growth culture directly if the sulfur and other toxins contents are low enough. The other option is to use concentrated CO_2 by purifying the flue gas using amine absorption. Some carbon dioxide pipelines are already in use but to accommodate the large volume from the power plants, purification of the flue gas into a more concentrated CO_2 stream may be desirable. The processed flue gas is transported from the power plant location to algae growth reactors.

Algae growth

The central component in this process system is the algae growth stage. In this model, four technology alternatives are considered in detail: OP, tubular photobioreactor (TPBR), bubble column photobioreactor (BPBR), and flat plate photobioreactor (FPBR). OP and closed PBRs have been analyzed in detail.[21–25] Closed photobioreactor offers some benefits in control and growth rates but are typically more expensive.[24] Life cycle analysis and experimentation of algae growth using tubular reactors has performed for production of specialty products at a much smaller scale than would be required for fuel production.[26] BPBRs are not as well-established and have never been tested seriously at large-scale, but they appear to have relatively low costs because of the simplicity in their design.

Because of the photosynthesized microalgae suspension in BPBRs, the sunlight irradiance from externally illuminated transparent wall to the core of the column declines. The volume of the photobioreactor can be demarcated into a dark interior core region and a relatively better illuminated peripheral region. Therefore, the column diameter is limited to a diameter that ensures the supply of enough sunlight irradiance.

OP (raceway) have historically been cheap that they are the go-to choice for large-scale production. However, significant drawbacks in perfecting growth in OP systems leave this issue open to debate.[27] In conditions favorable to growth, Davis[15] reported that PBRs were twice as expensive as OP per gallon of lipid extracted: \$3.99/gal for OP vs. \$6.62/gal for PBRs. In the case of the FPBR, productivities in a 2000-L reactor were given as 12 g dry cell mass/m^2/day.[28] As far as power is concerned, TPBRs are the most energy intensive. During photosynthesis of the algae growth, oxygen is produced which might be toxic to the algae if present at higher concentration. In closed PBRs, the power thresholds that are required to prevent unnecessary oxygen buildup between degassing stations are 53 W/m^3 for FPBR, 40 W/m^3 for BPBRs, and 2000 W/m^3 for TPBRs.[23]

In addition to choosing the right growth technology, algae can only grow when there is sufficient light, so there are design choices for what to do from dusk to dawn because there are constant emissions from the power plant. Light may be provided overnight for continuous growth via artificial lighting (LED). LEDs have narrow light emission spectra between 20 and 30 nm, which can be matched with the photosynthetic needs of the algae. The power consumption is 504 kWh per m^3 of reactor volume,[29] which will be a large power draw if implemented on a large scale. Because LED systems require a significant energy input, other options for dealing with the nighttime gas emissions might be more economically feasible.[29] During the night, the gas may be stored

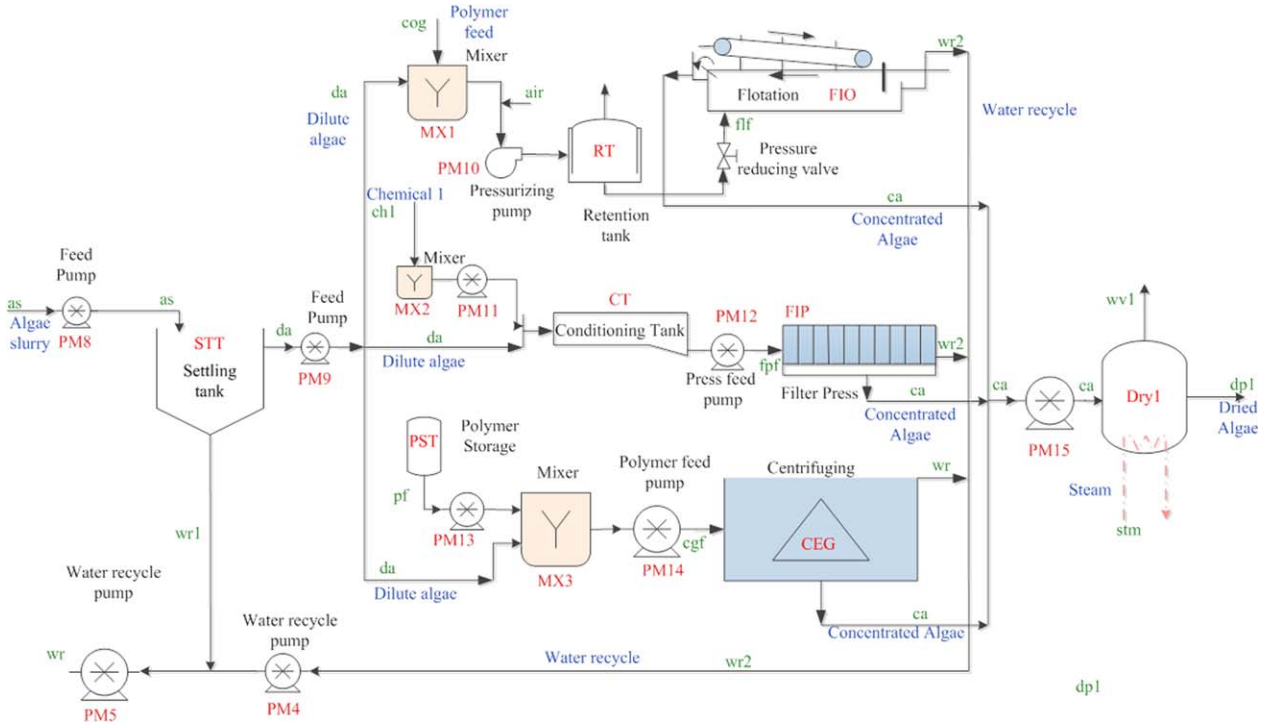

Figure 4. Process flow diagram of algae harvesting, dewatering and drying.

[Color figure can be viewed in the online issue, which is available at wileyonlinelibrary.com.]

in large, pressurized tanks or underground. Underground storage requires lots of energy and capital investment, but the gas can be stored at a higher pressure and at much higher volumes than conventional pressure vessels.[30] Conventional pressure vessels can accommodate a lower maximum pressure and lower volume but do not need as much compression power.[31] If the cost of storage is too large, the flue gas may be vented from the power plant which would mean that emission reduction and biofuel production would be limited to the day time.[29] There are tradeoffs in each of these options among greenhouse gas (GHG) emissions, power consumption, and system costs.

Algae species selection also plays a part in streamlining the process because there are many characteristics such as high growth rates, autoflocculation, size, environmental tolerances, and so forth that play a part in choosing the optimal algae species. In the Aquatic Species Program by the US Department of Energy, thousands of species were evaluated and several good options were identified.[32] The research indicates that the lipid content naturally ranges from 20 to 30% and under some conditions, it can rise to 70% or higher.[33] As more research is done on algae species, it is possible that a winner will be found that satisfies all or most of the desirable criteria, but for now there is not a consensus as to the best strain.

Harvesting, dewatering, and drying

After algae growth, to enhance the algal oil extraction, the dilute microalgal suspensions that may enter at concentrations of 0.02–0.06% total suspended solids (TSS) need to be concentrated to 15–25% TSS.[34] A primary harvesting step concentrates the algae around 10-fold in a settling tank. Dewatering is a crucial step in the downstream processing stage because the concentration of algae needs to be increased by close to a factor of a thousand and this can be very energy intensive especially because microalgae can be just a few microns.

As shown in Figure 4, three dewatering technology alternatives are considered: flotation thickening, filtration, and centrifugation. Flotation thickening is inexpensive but requires more drying than centrifugation or filtration because it only dries the dilute algae to 10% solid concentration.[35] Filtration returns a very dry product near 40% dry solids but requires heavy maintenance. Although centrifuges also return a relatively dry product (32%), they need a lot of power to keep running.[35] The water separated in the settling tank and from the dewatering unit is recycled back to the algae growth. In all cases, the algae must be dried to a final product using an expensive thermal drying process.

Lipid extraction and power generation

The lipids from the dried algae must then be extracted from the other algae components that include carbohydrates and proteins. This processing subsection is mainly composed of lipid extractor, lipid/hexane recovery, anaerobic digester, biogas upgrading, and gas turbine. Algal oil is extracted from the dried algae biomass stream using hexane as a solvent. The algal oil, or lipids, is further refined to hydrocarbon biofuels and the residue is digested in an anaerobic digester to produce a biogas mixture with 67% methane. The biogas is further upgraded using pressurized water and then burned to generate power that can be used in other processing sections.[36,37] The flue gas from the gas turbine is recycled back to the algae growth as shown in Figure 5.

Algal oil upgrading

Algal oil must be upgraded into biodiesel or green diesel to be used as liquid transportation fuels. We consider five alternative upgrading technologies that include algal oil hydroprocessing and four different transesterification processes.

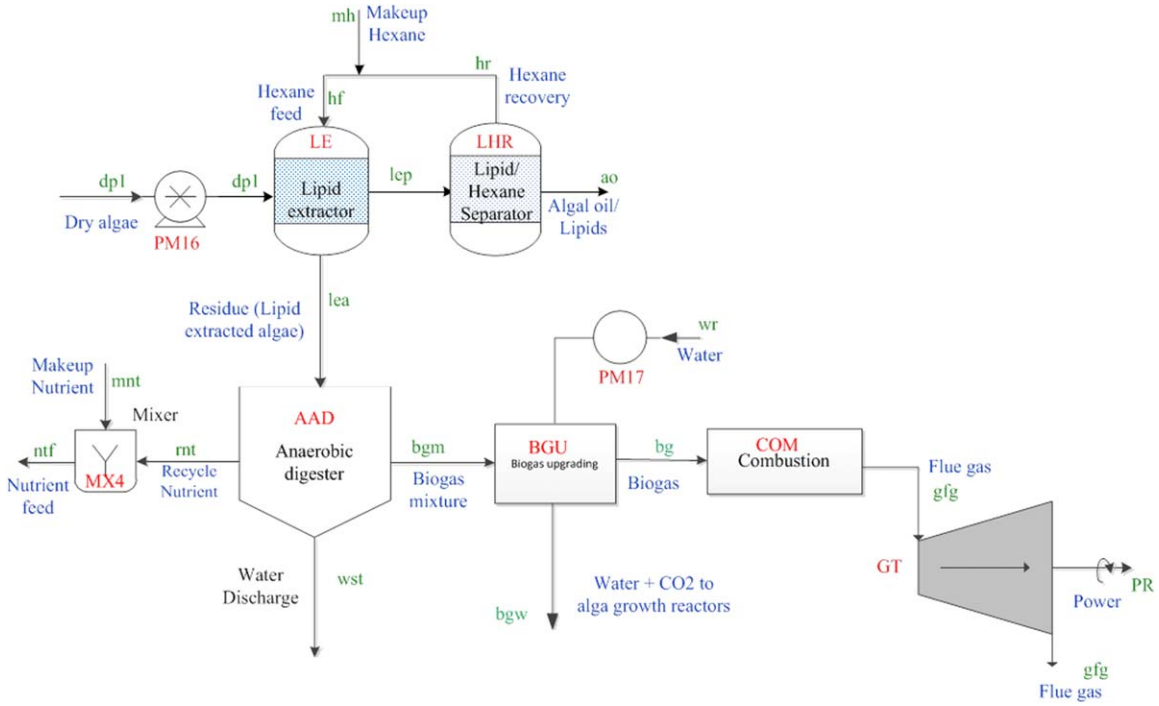

Figure 5. Lipid extraction, anaerobic digestion and gas turbine.

[Color figure can be viewed in the online issue, which is available at wileyonlinelibrary.com.]

The transesterification reaction converts algal oil to biodiesel.[38] Details on transesterification based on alkali-catalyzed transesterification can be viewed in the literature.[11,16] Biodiesel can be produced also from algal oil by transesterification in the presence of heterogeneous catalyst and enzyme catalyst.[39–41] The supercritical methanol transesterification produces biodiesel from the algal oil at supercritical condition in the absence of catalyst.[11,42] Hydroprocessing of algal oil is a relatively new technology that produces green diesel. Green diesel has a high cetane value, a lower gravity, good cold flow properties, and excellent storage stability. It is completely compatible for blending with the standard mix of petroleum-derived diesel fuels.[43,44]

Sodium methoxide-catalyzed transesterification. Sodium methoxide catalyst has the high conversion rate compared to related alkali-catalyzed transesterifications (Figure 6). The biodiesel yield from sodium methoxide-catalyzed transesterification of algal oil is dependent on the operating temperature; methanol-to-algal oil feed ratio, and the amount of catalyst. The algal oil enters the transesterification reactor

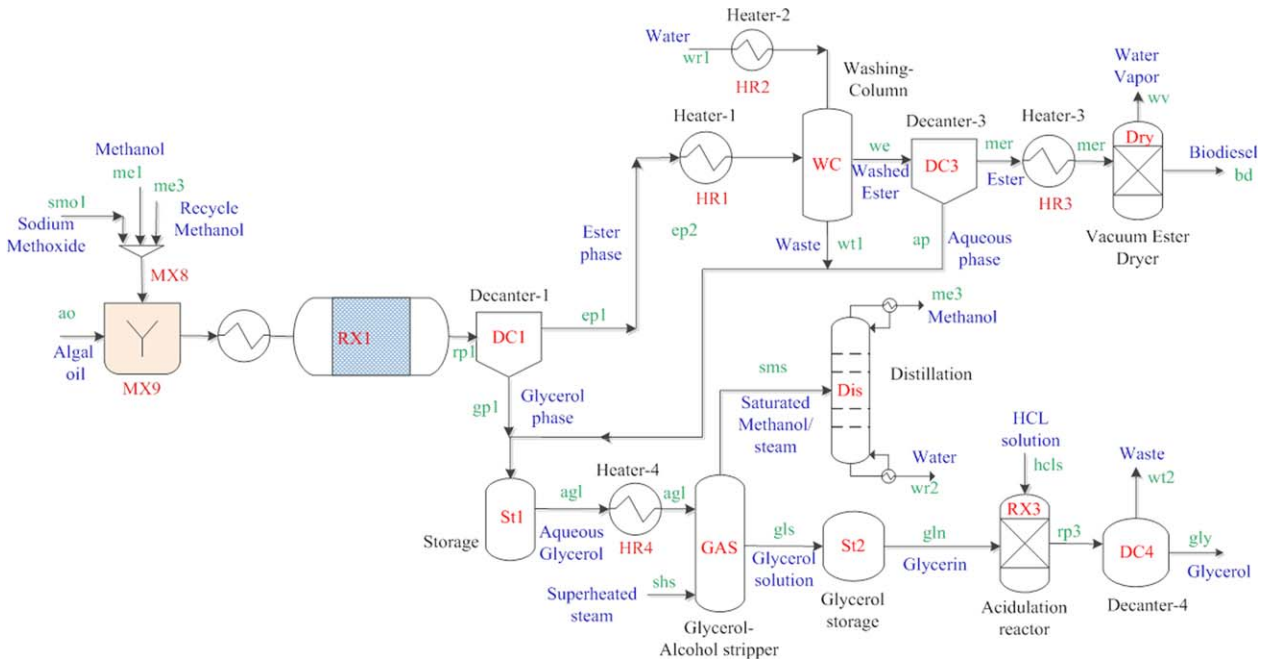

Figure 6. Sodium methoxide-catalyzed transesterification.

[Color figure can be viewed in the online issue, which is available at wileyonlinelibrary.com.]

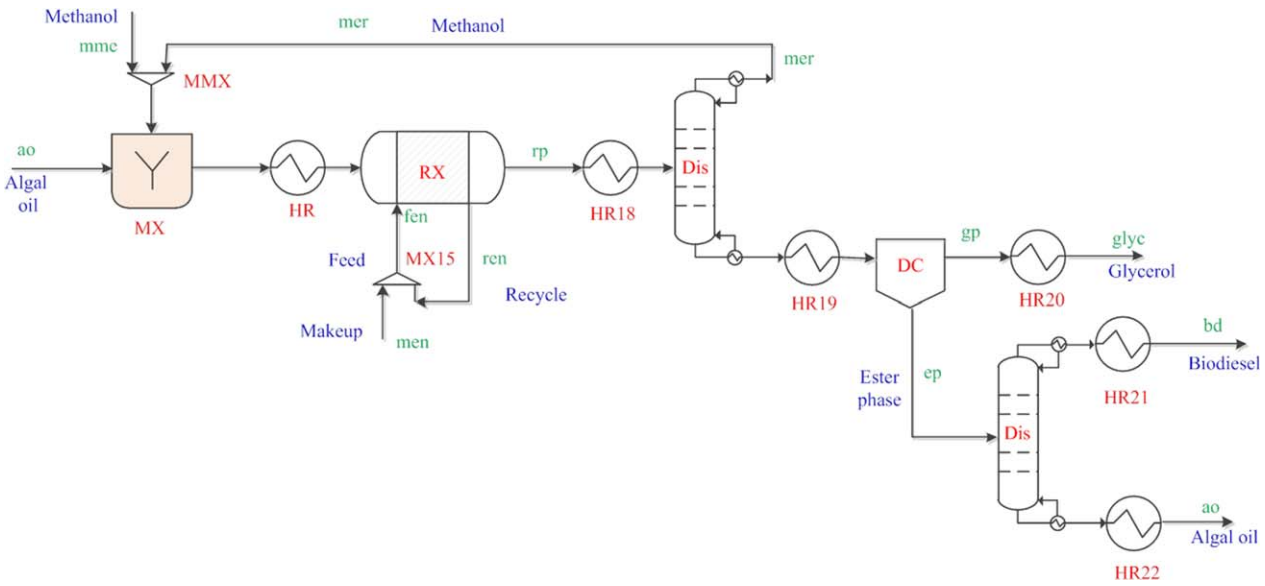

Figure 7. Process flow diagram for biodiesel production by enzyme catalyzed methanol, heterogeneous-catalyzed methanol, and enzyme-catalyzed transesterification.

[Color figure can be viewed in the online issue, which is available at wileyonlinelibrary.com.]

maintained at 60°C and atmospheric pressure. With 6 methanol-to-algal oil molar feed ratio, methanol is added to the reactor along with suitable amount of sodium methoxide catalyst. In the presence of the catalyst, transesterification between triglycerides and methanol takes place to form the methyl esters and glycerol as a byproduct. The remaining trace amount of free fatty acids (FFA) in the algal oil reacts with sodium methoxide to form soap and methanol. The reaction products are separated in decanter-1 to a glycerol-rich stream and methyl ester-rich stream. The glycerol phase goes to a temporary storage tank and the methyl ester phase is heated to 70°C before it goes to the methyl ester-washing column.[16,45]

Impurities in the methyl ester-rich stream, such as methanol, soaps, and free glycerol, must be separated from the methyl esters. This is accomplished by washing the methyl ester phase with softened water at 70°C. Use of countercurrent continuous wash columns helps minimize the amount of water needed.[46] The waste stream from the washing column is sent to the temporary storage tank, and methyl ester stream is sent to a settling tank. The remaining aqueous phase is separated from the methyl esters in the settling tank. The resulting methyl ester stream is then heated to 90°C before it is finally sent to the vacuum methyl ester dryer, under 35-mm Hg absolute pressure, to remove the remaining traces of moisture.

Glycerol-rich, the waste and the aqueous streams are combined in the temporary storage tank. The resulting stream is heated to normal boiling point of methanol (64.5°C). Methanol is stripped from the heated stream using superheated steam in the glycerol-alcohol stripper. The saturated methanol vapor and the steam are fed into a distillation column to recover pure methanol vapor as a distillate. The methanol vapor is condensed in a reflux condenser and is recycled back. The hot glycerol solution from the bottom of the stripper is sent to a glycerol holding tank. The crude glycerol from this holding tank is mixed with proper amounts of HCl solution in the acidulation reactor. Catalyst sodium methoxide in the stream reacts with HCl to form methanol and NaCl, and the soaps present in this stream react with HCl to form FFA and NaCl in the acidulation reactor. Using decanter-4, the FFA and other impurities such as the unreacted oil are separated from the glycerol-rich product.

Supercritical, heterogeneous, and enzyme-catalyzed transesterification. As shown in Figure 7, the three other methods of algal oil upgrading are modifications of the sodium methoxide-catalyzed transesterification process. These are supercritical methanol transesterification, heterogeneous-catalyst transesterification, and enzyme-catalyzed transesterification. The processes are quite similar to each other. So, it is necessary just to point out the difference among them.

In the supercritical methanol transesterification, first the algal oil is mixed with methanol, then the mixture is heated to 200–350°C,[47] and fed to the reactor. The methanol recovery distillation column purifies and recycles the methanol. The resulting mixture from the bottoms is further decanted into glycerol and methyl ester-rich streams. The methyl ester-rich stream is distilled into biodiesel and the unreacted algal oil-rich stream. The glycerol is somewhat valuable in its own right and may be sold as a side product.

The flow is the same for the other two methods, but instead of using supercritical methanol, the reaction is aided by the use of a catalyst. In heterogeneous-catalyzed transesterification, there is a recycle loop at the reactor that injects a catalyst of K_2CO_3/Al_2O_3. This allows the same separation steps described above. The catalyst is fed into the reactor at a 1–3% weight fraction for methyl ester formation at reaction temperature 60°C.[48]

In enzyme-catalyzed transesterification, the algal oil is mixed with methanol/tert-butanol mixture at a 0.55 volume fraction with respect to algal oil feed. The enzyme, lipase is fed to the reactor at a 4% fraction by weight. The enzyme is recycled and reused for 20 cycles. This high performance gives a 97% methyl ester yield at reaction temperature 50°C.[49]

Hydroprocessing. Production of biofuel via hydroprocessing gives a product chemically distinct from the biodiesel produced from the transesterification of algal oil

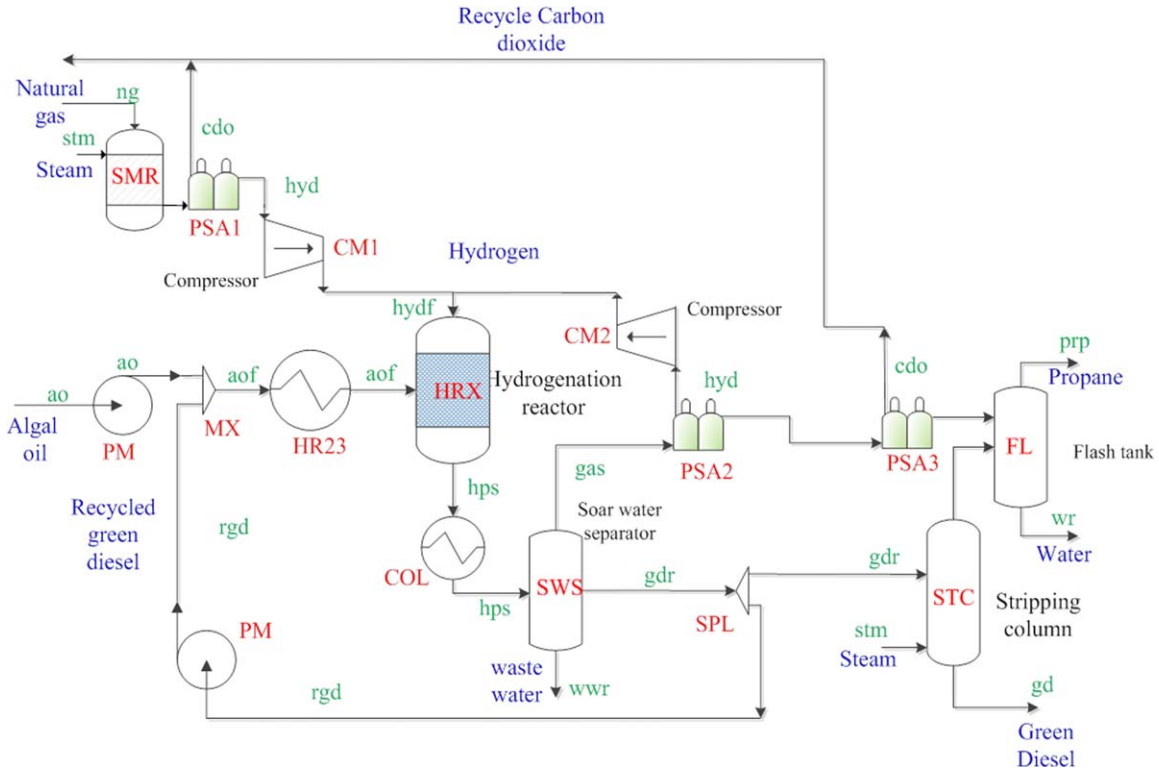

Figure 8. Steam methane reforming and Hydroprocessing.

[Color figure can be viewed in the online issue, which is available at wileyonlinelibrary.com.]

upgrading (Figure 8). Hydroprocessing produces "green diesel" which can be incorporated more easily into vehicle engines. The algal oil is first mixed with recycled green diesel of low quality and then fed to a hydrogenation reactor. This reactor requires excess amount of hydrogen representing a major cost factor in the system. Hydrogen is produced on site using steam methane reformer where steam and natural gas are reacted and the hydrogen gas produced is separated from CO_2 using PSA. The algal oil and hydrogen are reacted in the hydrogenation reactor at reactor temperature of 325°C and 34.5 bar pressure and yield mainly mixture of green diesel, carbon dioxide, water, propane, and unreacted hydrogen. The gases are separated in a soar water separator and much of the waste water is removed. The excess hydrogen is separated from the gas via PSA and recycled back to the hydrogenation reactor. Additionally, the carbon dioxide is separated from the gas stream via PSA and recycled back to the algae growth along with the carbon dioxide from the steam methane reformer, which allows for about 10% extra capacity in hydroprocessing. Some of the green diesel-rich stream is split off and mixed with the algal oil feed, while the rest is purified in a stripping column. The propane-rich stream from PSA is further purified in a flash tank and the residual water is removed.

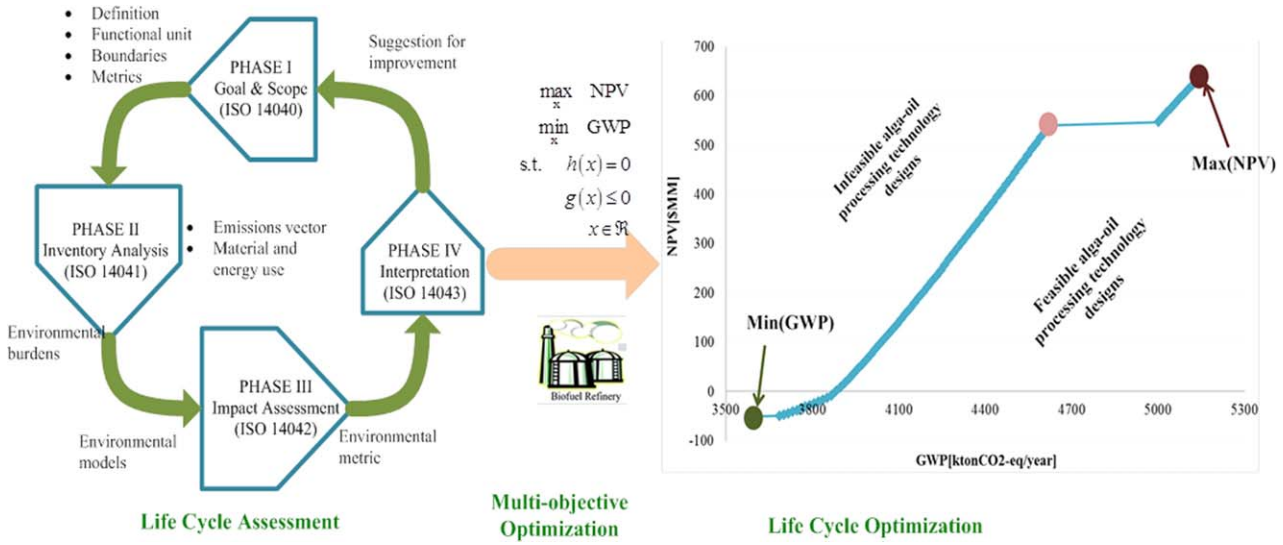

Figure 9. Coupling of life cycle assessment and multiobjective optimization.

[Color figure can be viewed in the online issue, which is available at wileyonlinelibrary.com.]

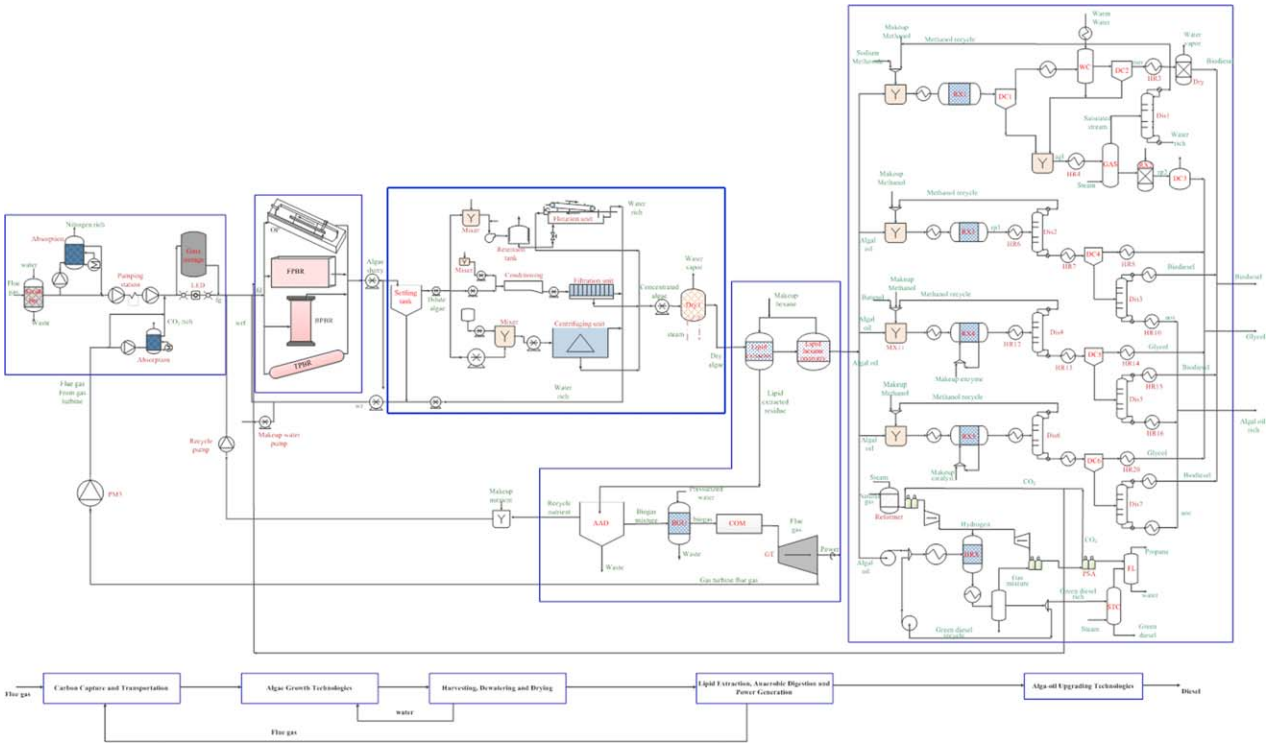

Figure 10. The proposed superstructure that includes carbon capture, gas transportation, algae growth, algae harvesting and dewatering, lipid extraction and algae-oil processing.

[Color figure can be viewed in the online issue, which is available at wileyonlinelibrary.com.]

Life Cycle Optimization Framework

Environmental performance assessment of the algae-based hydrocarbon biorefinery for simultaneous hydrocarbon biofuel production and carbon sequestration is conducted following the principles of LCA. General details on the LCA methodology can be found in Ref.[18]. The main goal of LCA is to provide quantitative environmental criteria for comparison among multiple feasible designs and operating conditions. However, LCA framework lacks a systematic way of generating feasible designs and operating conditions of the processing technologies. Hence to overcome such a drawback, LCA procedure is integrated with mathematical programming tools as shown in Figure 9 in such a way that LCA is used to assess the carbon sequestration and algae-based hydrocarbon biorefineries from the environmental perspective, while optimization techniques generate in a systematic way feasible technology alternatives, designs, and operating conditions and simultaneously identify the best designs in terms of economic performance and environmental impact.[50–52]

The calculation of the life cycle environmental impacts of the CCS and the algae-based hydrocarbon biorefineries follow the four LCA steps;[18] goal and scope definition; inventory analysis; impact assessment; and interpretation. These steps are explained below in the context of this work.

Goal and scope definition

The goal of the LCA analysis is to determine the life cycle environmental impact of the algae-based biorefinery. The functional unit of the LCA analysis is, therefore, production in terms of gallons of diesel. Considering the scope of this work, a cradle-to-gate analysis is performed that encompasses the environmental concern during the CO_2 separation, gas transportation, artificial lighting, the emissions associated with natural gas acquisition, electricity and heat consumptions, and direct emissions during the operation of the processing units from upstream to downstream. The environmental impact is quantified through the GWP metric. GWP is a relative scale which compares the global warming impact of a given chemical with that of the same mass of carbon dioxide whose GWP equals to 1 by convention.[53]

Inventory analysis

The inventory analysis step aims at inventory of input/output data associated with the CCS and the algae-based hydrocarbon biorefinery. The total life cycle emissions inventory accounts for the CO_2 separation, gas transportation, artificial lighting, and the emissions associated with natural gas acquisition, electricity and heat consumptions, and direct emissions during the operation of the processing units from upstream to downstream. The life cycle inventory entries per functional unit of the CO_2 purified, gas transported, artificial light requirement, the algae culture circulated, the steam, electricity and natural gas consumed, and the unit of direct emissions released should be obtained either from literature or by performing an LCA analysis on each source of emissions. The life cycle inventory entries can be retrieved from the standard environmental databases that store emission data associated with similar processes.[54–56] These parameters depend on the particular features of the emission sources (i.e., type of fuel used for steam generation and electricity mix).

Impact assessment

In this step, the life cycle inventory of emissions is translated into the corresponding contributions to environmental impact. GWP metric is used to quantify the environmental

concerns. It is determined as the sum of the GWP from direct emissions, emissions related to steam and electricity consumption during the operation of the CCS and the algae-based hydrocarbon biorefinery. The damage factor links the GWP with each GHG emissions of the CCS and the algae-based hydrocarbon biorefinery. The value of the global warming damage factors of the GHG emissions are reported in the intergovernmental panel on climate change (IPCC) publication.[53] The GWP is calculated over a specific time interval that must be stated, commonly 20, 100, and 500 years. IPCC 2007 framework that considers a time horizon of 100 years as part of the Kyoto Protocol[57] is adopted in this work.

Interpretation

In this step, the post optimization analysis of the optimal trade-off (Pareto curve) solutions (see Figure 9) of the multi-objective optimization problem is analyzed, and a set of conclusions and recommendations are formulated. The Pareto frontier represents the set of all the optimal solutions taking into account both economic and environmental objectives. All solutions below this curve are suboptimal solutions that the objective function values can be improved by using optimization methods. Any solution above this curve is infeasible, and the associated process alternative is impossible to achieve. This life cycle optimization approach provides further insights into the CCS and the algae-based hydrocarbon biorefinery design problem and allows a better understanding of the inherent trade-offs between the economic and environmental objectives.

Problem Statement

The superstructure of process network shown in Figure 10 demonstrates the configuration of capturing flue gas emissions from a coal fired power plant as a form of sequestration in algae, algae growth and harvesting, dewatering and drying of algae slurry, extraction of algal oil (lipid), biogas production and power generation, and processing of algal oil feedstock to biodiesel and green diesels. In the superstructure of the process network, the alternative technologies considered in this work include:

1. Flue gas: the use of either direct flue gas as carbon source of the algae growth or purified CO_2.

2. Algae growth: in this section, four different algae growth technologies are considered, namely, OP, TPBR, FPBR, and BPBR. Each type of photobioreactor technology has different productivity, power consumption, and algal slurry concentration.

3. Dewatering: the dewatering technology alternatives include flotation, filtration, and centrifuging. The main differences among the dewatering technologies are algae recovery percentage, concentration of algae, and power consumptions.

4. Algal oil upgrading: hydroprocessing and four transesterification technology alternatives are considered. Namely, sodium methoxide-catalyzed transesterification, supercritical methanol transesterification, enzyme-catalyzed transesterification, and heterogeneous-catalyzed transesterification. The algal biorefineries differ in their processing mechanisms, the type of catalyst, heat and power consumption, and the type of main and coproducts.

Moreover, alternatives among the use of artificial lighting during night time, temporary storage, and emitting the flue gas to the environment are considered.

In this superstructure optimization problem, the given parameters are the feed flue gas species mass fraction, capacity of the power plant, and split fraction of species in separation process units that does not involve reaction. Furthermore, the following parameters are independent to the process alternatives:

- Scrubber water feed to flue gas feed ratio.
- Flue gas transportation suction and discharge pressures.
- Hours of sun light per day.
- Unit of makeup solvent per CO_2 separated in monoethanolamine separation process.
- Lipid, protein, and carbohydrate percentage of algae.
- Excess air feed for combustion of biogas.
- The volumetric percentage of methane in the biogas.
- Fraction of methane recovery in biogas upgrading.
- Product distribution of anaerobic digester with respect to suspended solid feeds.
- Nutrient recovery fraction.
- Lipid extraction efficiency.
- Hexane ratio required for lipid extraction and hexane recycle ratio from hexane lipid recovery unit.
- Fraction of hexane loss with residue.
- Air fuel ratio of gas turbine combustion.
- Volumetric ratio of pressurized water to biogas feed.
- Algal oil species mass fraction.
- Molecular weights of species.
- Unit heat and power consumption of the processing units.
- Biogas to power conversion and generator efficiencies.
- Unit price of power, steam, natural gas, nutrient methanol, hexane, methylethanolamine, sodium methoxide, enzyme, catalyst, *t*-butanol, and water.
- Base case costs and mass flow rates of processing units.
- Cost scaling factor of each process unit.
- Life span of the technology in terms of years.
- Engineering supervision, construction, legal and contractors fee, project contingency, maintenance, and local tax and insurance factors are given as a percentage of the direct cost.
- Cost index to account for the purchase equipment cost inflation relative to current year.
- Selling price of the propane and glycerin side products.
- Life cycle inventory for each emission source category.
- Damage factor of the direct emissions that accounts for GWP relative to CO_2.
- Unit GWP contribution of power using the US electricity mix.
- Unit GWP contribution of steam using natural gas as steam generating source.

Parameters dependent on process alternatives

- Unit CO2 and water consumption depending on the algae growth technologies.
- Unit nutrient consumption per gram of algae growth.
- Productivity of algae growth technologies.
- Algae slurry concentration for each algae growth technology.
- Percentage of coagulants and polymer with respect to the algae mass feed to the dewatering technologies.
- Algae recovery and weight fraction in each dewatering technology.
- Rate of conversion and residence time of each reactant or product distribution.
- Stoichiometric coefficients of reacting species.

• Concentration of sodium methoxide in methanol, hydrochloric acid in water solution.
• Reaction rate of triglyceride and FFA.
• Methanol, t-butanol, sodium methoxide, catalyst, enzyme, hydrogen feed ratio with respect to the algal oil feed.
• Percentage of methyl ester washing water with respect to methyl ester feed.
• Percentage of hydrochloric acid solution with respect to glycerin feed.
• Product distribution of hydrogenation products.

The major assumptions are listed below

• Linear relationship between feed streams and heat and power consumptions of the process heat and electricity consuming units.

The goal is to obtain the optimal design of diesel processing technology by simultaneously maximizing the NPV and minimizing GWP, subject to design and operational constraints that include mass balances, energy balances, economic analysis constraints, and environmental impact assessment constraints by optimizing the following decision variables.

• Technology selection.
• Mass flow rates of species and streams.
• The flue gas emissions vented and consumed for algae growth.
• Heat and power consumption.
• Capital costs, operational costs, and revenue from side products.
• Environmental impacts in terms of GWP.
• Equipment capacity.
• Annual diesel production capacity.

Model Formulation

The mathematical model is formulated as a bicriteria MINLP problem which determines the optimal design and operation of the algae-based biorefinery considering the economic and environmental objectives. The economic objective is modeled as maximizing the NPV given by Eq. 35 subject to constraints (S1)–(S166) and Eqs. 1–34. The environmental impact objective is modeled as minimizing the GWP given by Eq. 41 subject to constraints (S1)–(S166) and (37)–(40). In the mathematical model formulation, four major types of constraints are considered, namely, mass balance constraints (S1)–(S.143), energy balance constraints (S144)–(S166), economic analysis constraints (1)–(35), and environmental impact analysis constraints (37)–(40). For the sake of limiting the length of the article, the details of the mass and energy balance on each unit operation and technology selection constraints are included in the Supporting Information. The detail economic and environmental impact-related constraints are presented below.

Economic analysis constraints

Capital cost estimation. ***Annualized project investment costs.*** The total project investment cost (apic) is given by the sum of the total annualized equipment purchase cost (apec), engineering cost, legal, and contractors fee, project contingency cost, land cost, and working capital cost. These costs are determined as a percentage of the annualized equipment purchase cost as shown below

$$\text{apic} = \text{apec}\,(1+K_{\text{ENG}}+K_{\text{LCF}}+K_{\text{PCC}}+K_{\text{LND}}+K_{\text{WCP}}) \quad (1)$$

where K_{ENG}, K_{LCF}, K_{PCC}, K_{LND}, and K_{WCP} are engineering cost, construction cost, legal, and contractors fee, project contingency factor, land cost, and working capital cost factors, respectively.

The total annualized equipment purchase cost is determined as the sum of the purchase cost of each unit involved in the process plant times the capital recovery factor (CRF) as shown below

$$\text{apec} = \text{CRF}\left(\sum_{l\in L_{\text{eq}}} \text{eic}_l\right)$$
$$L_{\text{eq}} \equiv \left\{\begin{matrix}\text{scr, ab1, pip, cm, ab2, led, gst, ag, pm4, pm5, pm8,}\\ \text{pm9, pm15, stt, dw, le, aad, bgu, pm17, gt, dpr}\end{matrix}\right\} \quad (2)$$

where eic_l is the purchase cost of equipment l in year of interest. CRF is determined as a function of the interest rate (IR) and the depreciation time of the project (T_{dp}) as shown in the equation below

$$\text{CRF} = \frac{\text{IR}\,(\text{IR}+1)^{T_{\text{dp}}}}{(\text{IR}+1)^{T_{\text{dp}}}-1} \quad (3)$$

The equipment purchase cost of unit l in the year of interest is determined as a function of the purchase cost (ecc_l) of the unit at the reference year (ref). We use Chemical Engineering Plant Cost Index (CEPCI)[58] to consider the inflation of the purchase equipment cost from the reference year as given by below

$$\text{eic}_l = \text{ecc}_l\left(\frac{\text{CEPCI}}{\text{CEPCI}_{\text{ref}}}\right) \quad \forall l \in L_{\text{eq}} \quad (4)$$

The purchase cost of each unit involved in the process plant at the reference year (ecc_l) is estimated via the following equations.

The purchase cost of each unit involved in the process plant in \$*MM* (ecc_l) is estimated via the equation below

$$\text{ecc}_l = \text{ECC}_b^l\left(\frac{m_f^l}{m_b^l}\right)^{sf^l} \quad \forall l \in L_{\text{eq}} \quad (5)$$

where m_f^l is the total flow rate of the fed to equipment l, m_b^l is the total inlet flow rate to equipment l in the base case, ECC_b^l is the purchase cost of equipment l in the base case, and sf^l is the sizing factor of equipment l. The set of equipment is given by

$$L_{\text{eq}} \equiv \{\text{scr, ab 1, ab 2, led, gst, pm 4, pm 5, pm 8, pm 9,}\ \text{pm15, dr 1, le, aad, bgu, pm 17, gt}\}$$

Gas transportation pipe cost is given by[59]

$$\text{ECC}_{\text{pip}} = \text{PRICE}_{\text{pip}}\sum_i l_i d_i \qquad i \in NC \quad (6)$$

where $PRICE_{pip}$ is the pipe capital cost in \$*MM* per m of pipe diameter per km of pipe length. l_i and d_i are pipe segment length and diameter in km and m, respectively.

The pumping station capital cost is determined as a function of the pumping power consumption as shown below[59]

$$\text{ECC}_{\text{pp}} = 7.84\,pr_{\text{pp}} + 0.46 \quad (7)$$

where pr_{pp} is the pumping power consumption in MW.

The purchase equipment cost of each algae growth technology is given by

$$\mathrm{ecc}^{\mathrm{ag}}_{\mathrm{agt}} = \mathrm{ECC}^{\mathrm{ag}}_{\mathrm{b,agt}} \left(\frac{m^{\mathrm{ag}}_{f,\mathrm{agt}}}{m^{\mathrm{ag}}_{\mathrm{b,agt}}} \right)^{sf^{agt}} \qquad \forall agt \in \{\mathrm{op}, \mathrm{tpbr}, \mathrm{bpbr}, \mathrm{fpbr}\} \tag{8}$$

where $m^{\mathrm{ag}}_{\mathrm{f,agt}}$ is the total flow rate of the fed to algae growth technology *agt*, $m^{\mathrm{ag}}_{\mathrm{b,agt}}$ is the total inlet flow rate to algae growth technology *agt* in the base case, $\mathrm{ECC}^{\mathrm{ag}}_{\mathrm{b,agt}}$ is the capital cost of photobioreactor *agt* in the base case, and sf^{agt} is the sizing factor of photobioreactor *agt*

$$\mathrm{ecc}_{\mathrm{ag}} = \sum_{\mathrm{agt}} \mathrm{ecc}^{\mathrm{ag}}_{\mathrm{agt}} \qquad \mathrm{agt} \in \{\mathrm{op}, \mathrm{tpbr}, \mathrm{bpbr}, \mathrm{fpbr}\} \tag{9}$$

The settling tank purchase cost is given as a function of the volumetric flow rate[35]

$$\mathrm{ecc}_{\mathrm{stt}} = 0.0785 q^{1.1}_{\mathrm{stt}} \tag{10}$$

where q_{stt} is the volumetric flow rate of the algae slurry fed to the settling tank in million gallon per day. The flow rate is determined as follows

$$q_{\mathrm{stt}} = \mathrm{CMGAL} \frac{\sum_{j \in \{wr,al\}} m^{\mathrm{stt}}_{\mathrm{fd,j}}}{\rho_{\mathrm{wr}}} \tag{11}$$

where CMGAL is a conversion factor from cubic meters to gallons.

The dewatering unit purchase cost is given by the following equations:

Equipment purchase cost of the flotation unit is modeled as a function of the volumetric flow rate of the dilute algae feed

$$\mathrm{ecc}^{\mathrm{dw}}_{\mathrm{flt}} = 0.0717 \left(q^{\mathrm{dw}}_{\mathrm{flt}} \right)^{1.14} \tag{12}$$

where q^{dw}_{flt} is the volumetric flow rate of the dilute algae fed to the dewatering technology *flt* in mgd. It is determined by

$$q^{\mathrm{dw}}_{\mathrm{dwt}} = \mathrm{CMGAL} \frac{\sum\limits_{j \in \{wr,al\}} m^{\mathrm{stt}}_{\mathrm{da,dwt,j}}}{\rho_{\mathrm{wr}}} \qquad \forall \mathrm{dwt} \in \{flt, fpt\} \tag{13}$$

The equipment purchase cost of the filtration unit is modeled as a function of the volumetric flow rate of the dilute algae fed

$$\mathrm{ecc}^{\mathrm{dw}}_{\mathrm{fpt}} = 0.0785 \left(q^{\mathrm{dw}}_{\mathrm{fp}t} \right)^{0.4535} \tag{14}$$

The equipment purchase cost of centrifuging unit is modeled as a function of the volumetric flow rate of the dilute algae feed

$$\mathrm{ecc}^{\mathrm{dw}}_{\mathrm{cgt}} = 0.0785\, q^{0.574}_{\mathrm{cgt}} \tag{15}$$

where $q^{\mathrm{dw}}_{\mathrm{cgt}}$ is the volumetric flow rate of the dilute algae fed to the centrifuge dewatering unit in m^3/h. $m^{\mathrm{stt}}_{\mathrm{da,cgt,j}}$ is in kton/day, and KGKT is a kilograms in a kilo-ton.

The volumetric flow rate of the dilute algae fed to the centrifuge dewatering unit is determined as a function of the feed mass flow rate and its density is shown below

$$q^{\mathrm{dw}}_{\mathrm{cgt}} = \mathrm{KGKT} \frac{\sum_{j \in \{wr,al\}} m^{\mathrm{stt}}_{\mathrm{da,cgt,j}}}{\mathrm{HD} \cdot \rho_{\mathrm{wr}}} \tag{16}$$

The equipment purchase cost of the dewatering technology is given by the purchase cost of the unit selected as shown below

$$\mathrm{ecc}_{\mathrm{dw}} = \sum_{\mathrm{dwt}} \mathrm{ecc}^{\mathrm{dw}}_{\mathrm{dwt}} \qquad d\mathrm{wt} \in \{\mathrm{flt}, \mathrm{fpt}, \mathrm{cgt}\}$$

The purchase equipment cost of the algal biorefinery reactor is given as a function of the volume of the reactor as shown below

$$\mathrm{ecc}^{l}_{\mathrm{bdpt}} = 0.015 \left(vr^{l}_{\mathrm{bdpt}} \right)^{0.55} \qquad \forall l \in \{rx1, rx3, rx4, rx5, rx6, hrx\}, \ \forall \mathrm{bdpt} \in \{\mathrm{noxtr}, \mathrm{sctr}, \mathrm{entr}, \mathrm{hetr}, \mathrm{hypro}\} \tag{17}$$

where vr^{l}_{bdpt} is the volume of reactor *l* of the biodiesel processing technology *bdpt* in m^3 and it is determined by

$$vr^{l}_{bdpt} = \frac{\tau^{l}_{\mathrm{bdpt}} q^{l}_{\mathrm{bdpt}}}{0.8} \qquad \forall l \in \{rx1, rx3, rx4, rx5, rx6, hrx\}, \ \forall \mathrm{bdpt} \in \{\mathrm{noxtr}, \mathrm{sctr}, \mathrm{entr}, \mathrm{hetr}, \mathrm{hypro}\} \tag{18}$$

where τ^{l}_{bdpt} and q^{l}_{bdpt} are the residence time in hours and feed volumetric flow rate in m^3/day, respectively. The feed volumetric flow rate is determined as

$$q_{\mathrm{bdpt}} = \mathrm{HD} \cdot \mathrm{TKG} \frac{m^{l}_{f,\mathrm{bdpt}}}{\rho^{l}_{f,\mathrm{bdpt}}} \qquad \forall l \in \{rx1, rx3, rx4, rx5, rx6, hrx\}, \ \forall \mathrm{bdpt} \in \{\mathrm{noxtr}, \mathrm{sctr}, \mathrm{entr}, \mathrm{hetr}, \mathrm{hypro}\} \tag{19}$$

where $m^{l}_{\mathrm{f,bdpt}}$ is the mass flow rate of the fed to reactor *l* in ton per hour and $\rho^{l}_{\mathrm{f,bdpt}}$ is the density of the feed in kg/m^3.

The equipment purchase costs of decanters are determined as shown in the equation below

$$\mathrm{ecc}^{\,l}_{\mathrm{bdpt}} = 0.0785 \left(q^{l}_{\mathrm{bdpt}} \right)^{1.1} \qquad \forall l \in \{dc1, dc3, dc4, dc5, dc6, dc7\} \ \forall \mathrm{bdpt} \in \{\mathrm{noxtr}, \mathrm{sctr}, \mathrm{entr}, \mathrm{hetr}, \mathrm{hypro}\} \tag{20}$$

where q^{l}_{bdpt} is the volumetric flow rate of the fed to decanted *l* in million gallon per day (mgd). It is determined as follows

$$q^{l}_{\mathrm{bdpt}} = \mathrm{CMGAL} \frac{m^{l}_{\mathrm{f,bdpt}}}{\rho^{l}_{\mathrm{f,bdpt}}} \qquad \forall l \in \{dc1, dc3, dc4, dc5, dc6, dc7\} \ \forall \mathrm{bdpt} \in \{\mathrm{noxtr}, \mathrm{sctr}, \mathrm{entr}, \mathrm{hetr}, \mathrm{hypro}\} \tag{21}$$

where $m^{l}_{\mathrm{f,bdpt}}$ is the mass flow rate of the fed to decanter *l* in ton per hour and $\rho^{l}_{\mathrm{f,bdpt}}$ is the density of the feed in m^3/kg.

The equipment purchase cost of other units of the algal biorefinery technologies are given by

$$\mathrm{ecc}^{\,l}_{\mathrm{bdpt}} = \mathrm{ECC}^{\,l}_{\mathrm{b,bdpt}} \left(\frac{m^{l}_{\mathrm{f,bdpt}}}{m^{l}_{\mathrm{b,bdpt}}} \right)^{sf^{l}_{bdpt}} \qquad \forall l \in L_{\mathrm{eq}}, \mathrm{bdpt} \in \{\mathrm{noxtr}, \mathrm{sctr}, \mathrm{entr}, \mathrm{hetr}, \mathrm{hypro}\} \tag{22}$$

where m^{l}_{f} is the total flow rate of the fed to unit *l*, m^{l}_{b} is the total inlet flow rate to unit *l* in the base case, $\mathrm{ECC}^{\,l}_{b}$ is the purchase cost of unit *l* in the base case, and sf^{l}_{bdpt} is the sizing factor of unit *l*. The set of units is given by

$$L_{\text{eq}} \equiv \{\text{dis}\,1, \text{dr}\,2, \text{st}\,1, \text{wc}\,, \text{gas}\,, \text{dism}, \text{disd}, \text{smr}, \text{hrx}, \text{cm1}, \text{cm2}, \text{psa}, \text{sws}, \text{stc}, f\}$$

Operating cost estimation. ***Total Annual Operating Cost.*** The total annual operating cost (aoc) of the carbon capture, algae growth, harvesting, dewatering and drying, algal oil extraction, anaerobic digestion, power generation, and algal oil upgrading is given by the sum of the fixed O&M cost (*fixc*), markup monoethanolamine (MEA) solvent cost (opc_{mmea}), makeup nutrient cost (opc_{mnt}), cost of makeup water (opc_{mwr}), makeup hexane solvent cost (opc_{mhex}), methanol feed cost (opc_{mme}), utility cost steam (*qhc*), natural gas (opc_{ng}), and power (*prc*) and catalyst and chemicals cost (opc_{ctch}) as shown in the equation below

$$\begin{aligned} &\text{aoc} = \text{fixc} + \text{qhc} + \text{prc} + \sum_j \text{opc}_j \\ &j \equiv \{\text{ng}, \text{ctch}, \text{mmea}, \text{mnt}, \text{mwr}, \text{mhex}, \text{mme}\} \end{aligned} \tag{23}$$

where j represents the species consumed, *fixc* is the given as the percentage (K_{OM}) of the total investment cost as shown below

$$fixc = K_{\text{OM}}\, apic \tag{24}$$

The annual power and steam consumption costs are determined by the equations below

$$\text{prc} = T_{\text{op}}\, \text{PRICE}_{\text{pr}} \left(\sum_{l \in L_{eq}} pr_l - \text{prg}_{\text{gt}} \right) \tag{25}$$

$$\text{qhc} = T_{\text{op}}\, \text{PRICE}_{\text{qh}} \sum_{l \in L_{eqp}} qh_l \tag{26}$$

where PRICE_{pr} is the unit cost of power in \$/kWh and PRICE_{qh} is unit cost of steam in \$/kWh, pr_l and qh_l are the annual power and steam consumption of unit l in MW, respectively. T_{op} is the annual operating hours.

Annual cost of species j consumed is determined as a function of unit price and annual consumption of the species

$$\begin{aligned} &\text{opc}_j = \text{PRICE}_j m_j T_{op} \\ &\forall j \in \{\text{ng}, \text{ctch}, \text{mmea}, \text{mnt}, \text{mwr}, \text{mhex}, \text{mme}\} \end{aligned} \tag{27}$$

where $\text{PRICE}_j$is the unit price of species j, and m_j is the mass flow rate of species j consumed.

Total *annual cost estimation.* The total annual cost is given by the sum of annualized project investment cost and annual operational cost

$$\text{tac} = \text{apic} + \text{aoc} \tag{28}$$

Annual production rates in million gallons of diesel and coproducts are determined as a function of the mass flow rates of the species produced per day, operating hours per year, and density of the species

$$\begin{aligned} v_j = \frac{\text{TKG} \cdot \text{CMG}}{\text{GMG}} \frac{\sum_{\text{bdpt}} m_{\text{bdpt},j}}{\rho_j} T_{\text{op}} \quad &\forall j \in \{\text{bd}, \text{glyc}, \text{gd}, \text{prop}\}, \\ &\text{bdpt} \in \{\text{noxtr}, \text{sctr}, \text{entr}, \text{hetr}, \text{hypro}\} \end{aligned} \tag{29}$$

where v_j is the annual production of species j in million gallons. $m_{\text{bdpt},j}$ is the mass flow rate of species j produced in ton per day. CMGAL is the unit conversion from cubic meters to gallons and *GMG* is the conversion from gallons to millions of gallons.

Net present value. ***Revenue.*** The revenue from selling diesel and the side products are given by Eq. 30

$$\text{Rev} = \sum_{j \in \{\text{gd,bd,prop,gly}\}} \text{PRICE}_j v_j \tag{30}$$

where v_j is the annual production of diesel and side product j in MM gallon, and $PRICE_j$ is the market price of the diesel and side product j in \$/gal.

Two types of government incentives, volumetric incentive for biodiesel production through the Commodity Credit Corporation (INCV) and biorefinery construction state incentive (INCC)[60] are considered. The volumetric incentive is determined via

$$\text{INCV} = \text{VI}_{\text{inc}} \sum_{j \in \{gd,bd\}} v_j \tag{31}$$

where VI_{inc} is the unit price of volumetric incentive in \$/gal of diesel produced. For biorefinery construction, the government incentive received for construction should be less than a certain percentage (*INCP*) of total capital investment and maximum allowable incentive (*INCM*).[60] The definition of such incentives is given by the following two constraints[61–63]

$$\text{INCC} \leq \text{INCP} \cdot \text{TPIC} \tag{32}$$

$$\text{INCC} \leq \text{INCM} \tag{33}$$

Constraint (32) guarantees that government incentives will be 0 if the biorefinery is not constructed.

The annual gross profit (AGP) and annual actual profits after tax (*APAT*) are given by Eqs. 34 and 35, respectively

$$\text{AGP} = \text{Rev} - \text{TAC} \tag{34}$$

$$\text{APAT} = (1 - R_{\text{tax}})\text{AGP} + \text{INCV} \tag{35}$$

where R_{tax} is the tax rate.

Net Present Value. The economic objective function is formulated in terms of the NPV. After discounting the net income in all years to the starting point of the project, the NPV is obtained by Eq. 36

$$\text{NPV} = -T_{ls}\text{apic} + \text{INCC} + \sum_{t \in T_{ls}} \frac{\text{APAT}}{(1+r)^t} \tag{36}$$

where r is the annual discount rate, T_{ls} is the life span of the project, and t is the order of the time period.

The economic performance objective function model is given as follows

$$\begin{aligned} &\max_{x,y} \quad \text{NPV} \\ \text{s.t.} \quad &h(x,y) = 0 \\ &g(x,y) \leq 0 \\ &\sum_j y_{i,j} = 1 \qquad \forall i \in \{\text{sections}\}, j \in \{\text{technology alternatives}\} \\ &x \in \Re, y \in \{0,1\} \end{aligned} \tag{37}$$

where NPV denotes the economic performances objective function of the algae-based biorefinery. The continuous variables x represents decision variables such as flow rates, unit capacity, heat consumption, power consumption, investment cost, operational cost, revenue, and so forth. The binary

variables are denoted by y, representing selection of technology j of the algae-based biorefinery processing section i. The equality constraints $h(x,y) = 0$ represents linear and nonlinear functions of the mass and energy balance relations and the economic analysis-related equality functions. On the other hand, the inequality constraints $g(x,y) \leq 0$ represent the design specifications, such as minimum and maximum equipment capacities and upper and lower limits on process variables.

Environmental impact-related constraints

In this work, the environmental impact of the algae-based biorefinery is modeled following the principles of LCA. The details on the LCA steps are discussed in Section Life Cycle Optimization Framework and the constraints related to the environmental impact analysis are presented below.

The source of the environmental impact is categorized in three subclasses. Environmental impact related to the direct emissions from the processing plant ($\text{gwp}_{\text{demis}}$), emissions related to the power (gwp_{pr}), and heat (gwp_{qh}) consumptions of the biorefinery during its operation.

GWP direct emissions. The life cycle direct emissions inventory ($\text{LCI}_b^{\text{emiss}}$) associated with the algal biorefinery accounts for the emissions from the monoethanolamine absorptions (LCI_b^{ab1} and LCI_b^{ab2}), the direct vents of the flue gas from the power plant (LCI_b^{vent}), gas degassed from algae growth (LCI_b^{ag}), and anaerobic digester waste ($\text{LCI}_b^{\text{aad}}$) as shown in the equation below

$$\text{LCI}_b^{\text{emiss}} = \text{LCI}_b^{ab1} + \text{LCI}_b^{ab2} + \text{LCI}_b^{ag} + \text{LCI}_b^{\text{aad}} \tag{38}$$

The direct emissions inventory is translated to the GWP contribution as a function of the damage factor and the inventory entries as shown below

$$\text{gwp}_{\text{demis}} = \phi_b \text{LCI}_b^{\text{emiss}} \tag{39}$$

where the parameter ϕ_b is the damage factor that accounts for the GWP associated with the direct emissions of GHG b.

GWP power consumption. The power consumption associated with the operation of the CO_2 sequestration and algae-based hydrocarbon biorefinery is given by the sum of the power consumption of the scrubber, monoethanolamine absorptions, artificial lighting, pumping stations, algae growth, dewatering unit, lipid extraction, anaerobic digestion, nutrient recycle, and the algal oil upgrading. Therefore, the GWP contribution from power consumption is determined as shown below

$$\begin{aligned} &\text{gwp}_{\text{pr}} = \theta_{\text{pr}} \sum_k p\text{r}_{\text{k}} \\ &\forall k \in \{\text{scr}, \text{ab1}, \text{pp}, \text{ab2}, \text{led}, \text{ag}, \text{pm}, \text{dw}, \text{lep}, \text{aad}, \text{rnt}, \text{bd}\} \end{aligned} \tag{40}$$

where the parameter θ_{pr} is the damage factor that accounts for the GWP associated with power generation retrieved using the electricity mix of the U.S.

GWP heat consumption. The heat consumptions associated with the operation of the algal biorefinery is given by the sum of the heat consumption of the monoethanolamine absorptions, pumping stations, algae drying, lipid extraction, anaerobic digestion, and biogas upgrading and algal oil upgrading. Therefore, the GWP contribution from heat consumption is determined via the following equation

$$\text{gwp}_{\text{qh}} = \theta_{qh} \sum_k qh_k \qquad \forall k \in \{ab1, pp, ab2, dr1, le, aad, bgu, bd\} \tag{41}$$

where the parameter θ_{qh} is the damage factor that accounts for the GWP contribution associated with the heat consumption by assuming the heat is generated using natural gas as the primary energy source.

The total GWP contribution is given by the sum of the GWP contributions from the direct emissions, power and heat consumptions as shown below

$$\text{gwp} = \sum_k \text{gw}\, p_k \qquad \forall k \in \{\text{emiss}, \text{pr}, \text{qh}\} \tag{42}$$

The environmental performance measure objective function model is given as follows

$$\begin{aligned} &\min_{\text{x,y}} \quad \text{GWP} \\ \text{s.t.} \quad &h(x,y) = 0 \\ &g(x,y) \leq 0 \\ &\sum_j y_{i,j} = 1 \qquad \forall i \in \{\text{sections}\},\ j \in \{\text{technology alternatives}\} \\ &x \in \Re, y \in \{0,1\} \end{aligned} \tag{43}$$

where GWP denotes the environmental performances objective function of the biorefinery. The continuous variables x represents decision variables such as flow rates, unit capacity, heat and power consumptions, life cycle emissions inventory, direct emissions, indirect emissions, and so forth. The binary variables are denoted by y representing selection of technology j in algae-based biorefinery processing section i. The equality constraints $h(x,y) = 0$ denotes linear and nonlinear equality functions that represent the mass and energy balances, and LCA calculations. The inequality constraints $g(x,y) \leq 0$ represents the design specifications, such as minimum and maximum equipment capacities and upper and lower limits on process variables.

Solution Algorithm

The combined use of LCA and multiobjective optimization is a suitable framework for identifying opportunities for economic and environmental improvements in a rigorous and systematic manner.[17,50] In this regard, the multiobjective optimization problem is formulated by combining the economic performance and the environmental impact objective functions given by Eqs. 36 and 42, respectively, subject to constraints (S1)–(S166), Eqs. 1–35, and Eqs. 38–41. The resulting model is an MINLP Eq. 44 with the integer variable constraints to ensure the selection of one type of CO_2 gas feed by Eq. S5, algae growth technology by Eq. S22, dewatering technology by Eq. S37, and algal oil upgrading processing technology by Eq. S74. The nonlinear terms arises from Eqs. 5, 8, 10, 12, 14, 15, 17, 20, and 22

$$\begin{aligned} (\text{M1}) \quad &\max_{\text{x,y}} \quad \text{NPV} \\ &\min_{\text{x,y}} \quad \text{GWP} \\ \text{s.t.} \quad &h(x,y) = 0 \\ &g(x,y) \leq 0 \\ &\sum_j y_{i,j} = 1 \qquad \forall i \in \{\text{sections}\}, j \in \{\text{technology alternatives}\} \\ &x \in \Re, y \in \{0,1\} \end{aligned} \tag{44}$$

M1 is an MINLP problem with nonlinear and nonconvex constraints. Solving such large-scale problem using commercially available global optimizer BARON[64] can be expensive. Another alternative to solve the MINLP problem is to use the local solvers that rely on the convexity assumptions which are highly dependent on the starting point. Therefore, to obtain a good-quality feasible initial point, we propose a two-stage heuristic solution algorithm to solve the resulting nonconvex MINLP model.[65] In the first stage, the original MINLP model (M1) is reformulated into an MILP problem by introducing a piecewise linear approximation for each nonlinear and nonconvex terms.[66] The MILP model is then solved to obtain a good-quality feasible solution that used as a starting point for solving the MINLP model using local solvers.

Piecewise linear approximation

The equipment purchase cost-related functions are nonlinear and nonconvex functions. To linearize the equipment purchase cost-related nonlinear functions given in Eqs. 5, 8, 10, 12, 14, 15, 17, 20, and 22, we adopt a piecewise linear approximation[66,67] considering 100 intervals per nonlinear term. Let $P \equiv \{1,2,3,....p\}$ denotes the set of intervals in the piecewise linear function of $ec(mr_l)$, the lower and upper bounds of the mass flow rate ratio (mr_l) between the base case ($m_{b,l}$) and the actual design (m_l) of equipment l for each interval are given by $U_{l,0}, U_{l,1}, U_{l,2}, ..., U_{l,p}$, respectively

$$\mathrm{ec}\,(mr_l) = \sum_{p\in P} \left(a_{l,p} w_{l,p} + b_{l,p} y_{l,p}\right) \qquad \forall l \in l_{eq} \tag{45}$$

$$\sum_{p\in P} y_{l,p} = 1 \qquad \forall l \in l_{eq} \tag{46}$$

$$mr_l = \sum_{p\in P} w_{l,p} \qquad \forall l \in l_{eq} \tag{47}$$

$$U_{l,p-1} y_{l,p} \le w_{l,p} \le U_{l,p} y_{l,p} \qquad \forall l \in l_{eq},\ p \in P \tag{48}$$

$$y_{l,p} \in \{0,1\}, \qquad w_{j,p} \ge 0 \ \ \forall l \in l_{eq},\ \ p \in P \tag{49}$$

$$a_{l,p} = \frac{(U_{l,p})^{sf_l} - (U_{l,p-1})^{sf_l}}{U_{l,p} - U_{l,p-1}}, \qquad b_{l,p} = (U_{l,p})^{sf_l} - a_{l,p} U_{l,p},\ \forall l \in l_{eq},\ p \in P \tag{50}$$

where $ec(mr_l)$ is the approximated equipment purchase cost and mr_l is the mass flow rate ratio between the base case ($m_{b,l}$) and the actual design (m_l) of equipment l.

Therefore, the original MINLP (M1) is transformed to an MILP (M2) model through piecewise linearization approximations as shown in Eq. 51

$$\begin{aligned}
(\mathrm{M2}) \quad & \max_{x,y} && \mathrm{NPV} \\
& \min_{x,y} && \mathrm{GWP} \\
\mathrm{s.t.} \quad & h(x,y) = 0 && \\
& g(x,y) \le 0 && \\
& \sum_j y_{i,j} = 1 && \forall i \in \{\text{sections}\}, j \in \{\text{technology alternatives}\} \\
& x \in \Re, y \in \{0,1\} &&
\end{aligned} \tag{51}$$

Where the equality constraints $h(x,y) = 0$ denotes linear equality functions that represent the mass and energy balances, the economic analysis-related equality functions, and LCA calculations.

Heuristic algorithm

Step 1: Solve the MILP model (M2).

Step 2: Solve the MINLP model (M1) using MINLP solvers that relay on convexity assumptions using the optimal values of continues and discrete variables from Step 1 as the initial values.

NOTE *If we solve problem (M2) with the proposed two-stage algorithm by using an MINLP local solvers such as DICOPT and Simple Branch and Bound (SBB), the optimal solution may not be globally optimal. However, the optimal solution still has all the binary variables at integer value. Besides, the solution obtained from the heuristic algorithm for problem (M2) is also a feasible solution of problem (M1).*

ε-Constraint method

The solution to the bicriteria optimization problem is given by a set of Pareto optimal points. In this work, to obtain the Pareto curve, ε-constraint method[68] is implemented. The ε-constraint method formulates an auxiliary scalar optimization problem by transforming one of the objective functions into additional constraints. To generate the Pareto curve, first the problem is solved for each scalar objective function so as to obtain the lower and upper limits of the search interval within which all ε values fall. Specifically, the lower bound of GWP is obtained by minimizing Eq. 42 subject to constraints (S1)—(S166), and Eqs. 38–41. We solve an optimization problem with constraints (S1)–(S166), and (1)–(35), to obtain the upper bound with the following objective function

$$\max : \mathrm{NPV} - \chi \cdot \mathrm{GWP} \tag{52}$$

where χ is a very small value, for example, 0.0001. The next step is partitioning the interval into equal subintervals. Finally, each limit of the subintervals is introduced as an upper bound for the individual iteration to generate the optimal trade-off designs, with the objective of maximizing Eq. 36 and adding the following constraint

$$\mathrm{GWP} \le \varepsilon \tag{53}$$

Finally, the optimal trade-off designs of the proposed bicriteria MILP model is obtained along with the optimal solutions for different values of GWP.

Results and Discussions

The parameter values for the algae strain that include the algae (*Haematococcus pluviaslis*) productivity, *H. pluviaslis* composition (lipids:proteins:carbohydrates) and algae recovery and concentration, reaction rates, residence time, unit cost of raw materials, utilities, base case cost and capacity, and other parameters can be viewed in the Supporting Information. To simplify the discussion, we assumed the diesel prices \$10/gal for biodiesel and \$10.5/gal for green diesel, which are higher than the current unit prices, so as to result a positive NPV. To capture the dependency of the model results on the diesel prices, sensitivity analysis is performed, and the Pareto solutions of the sensitivity analysis are presented in Section Sensitivity analysis.

The multiobjective MNILP problem is modeled in GAMS 23.9.[69] All the computational studies are performed on a Dell Optiplex790 Desktop with Intel® Core™ *i*5–2400, 3.10-GHz CPU, and 8-GB RAM. The MILP (M2) model is

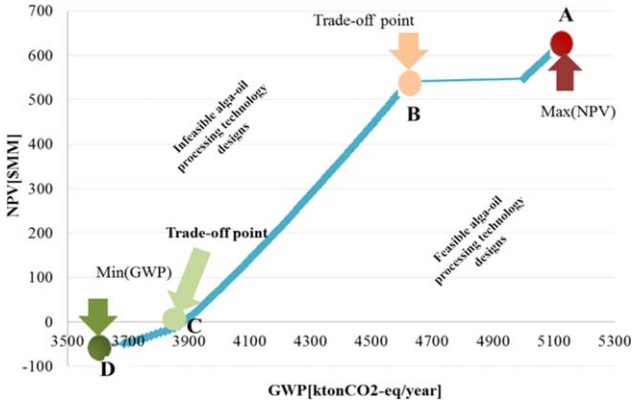

Figure 11. Pareto curve for optimal solutions.

[Color figure can be viewed in the online issue, which is available at wileyonlinelibrary.com.]

solved using CPLEX 12.4.1 and the resulting MILP optimization problem includes 13,199 constraints, and 7347 continuous and 5614 discrete variables in which 14 of them represent the technology selection and the remained came from the piecewise linear approximation. The MINLP model is solved with DICOPT 23.9.1 and the resulting MINLP optimization problem includes 1887 constraints, and 1747 continuous and 14 discrete variables.

Pareto curve

The Pareto-optimal curve of the bicriteria superstructure optimization problem is obtained following ε-constraint method. The entire solution process takes a total of 50.5 CPU-s for all 100 Pareto points. The resulting Pareto curve is given in Figure 11. All the optimal trade-off solutions of the model that take into account the technology selections, the economic, and environmental objectives lie on the Pareto curve. Hence, the solutions below the Pareto frontier of Figure 11 are suboptimal solutions, and any solution above this Pareto curve is infeasible.

The resulting Pareto curve shown in Figure 11 demonstrates the trade-off between the NPV and GWP. The y axis of the Pareto curve represents NPV and x axis represents GWP. The GWP presented in the curve is based on the cradle-to-gate LCA analysis. The GWP ranges from 5112 to 3610 $ktonCO_{2\text{-eq}}$ per year. Similarly, the NPV of the Pareto solutions ranges from \$624 to −50.32 MM. Four Pareto optimal solutions are selected from the curve for analysis of the results. Point A is the maximum NPV solution and corresponds to the maximum green diesel production and GWP. Point B represents a design that corresponds to the maximum capacity of biodiesel production based on transesterification of algal oil. This point is an important one that shows the shift from hydroprocessing technology to the sodium methoxide-catalyzed transesterification technology. Point C represents another important trade-off design where the photobioreactor and dewatering technologies are shifted from TPBR to BPBR and from filtration dewatering technology to flotation technology, respectively. Point D is the minimum GWP design and the GWP is mainly from of the power plant direct emissions. As shown in Figure 11, the environmental impact and the NPV are decreasing in the direction from Pareto point A to D. In the same direction, the direct flue gas vent increases which leads to the decrease in the capacity of the algae biomass harvesting and consequently decreases the biofuel production.

The results show that the higher the NPV, the higher total GWP will be. This can be explained that as the diesel production increases, the revenue increases and hence the NPV. As the biofuel production increases, the CO_2 direct emissions decrease because the CO_2 emissions are the main source of carbon for the biofuel production. However, the GWP contributions due to power and heat consumptions also increase as the capacity of the algal biorefinery increases. As a result, the overall GWP increases. The diesel production amount at the selected Pareto points A, B, C, and D are 47.12 MM gal/year, 43.12 MM gal/year, 6.83 MM gal/year, and 0.07 MM gal/year, respectively. The corresponding production costs are \$6.33, \$6.34, \$6.57, and \$77.8 per gallon of diesel, respectively. The high cost of the last point is due to the fact that nearly no biodiesel is produced so little revenue is generated to recoup the high fixed investment costs.

Point A: The maximum NPV case involves a large production close to 48 million gallons per year. The optimal process design for this maximum NPV shown in Figure 12 includes the use of direct flue gas from the power plant, the use of artificial lighting, TPBR, filter press dewatering unit, and algal oil upgrading via hydroprocessing. The higher productivity using the hydroprocessing technology is made possible by the additional carbon dioxide emissions recycled from the steam methane reformer and the CO_2 from the hydrogenation reactor gas products of the hydroprocessing

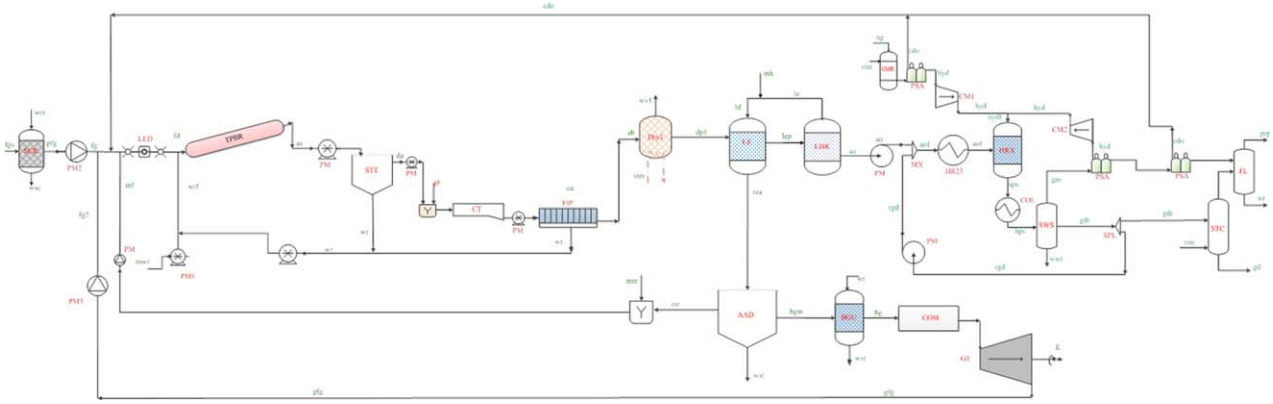

Figure 12. Maximum NPV optimum process design includes carbon capture, gas transportation, tubular photobioreactor, filter press dewatering unit, lipid extraction and hydroprocessing conversion pathways.

[Color figure can be viewed in the online issue, which is available at wileyonlinelibrary.com.]

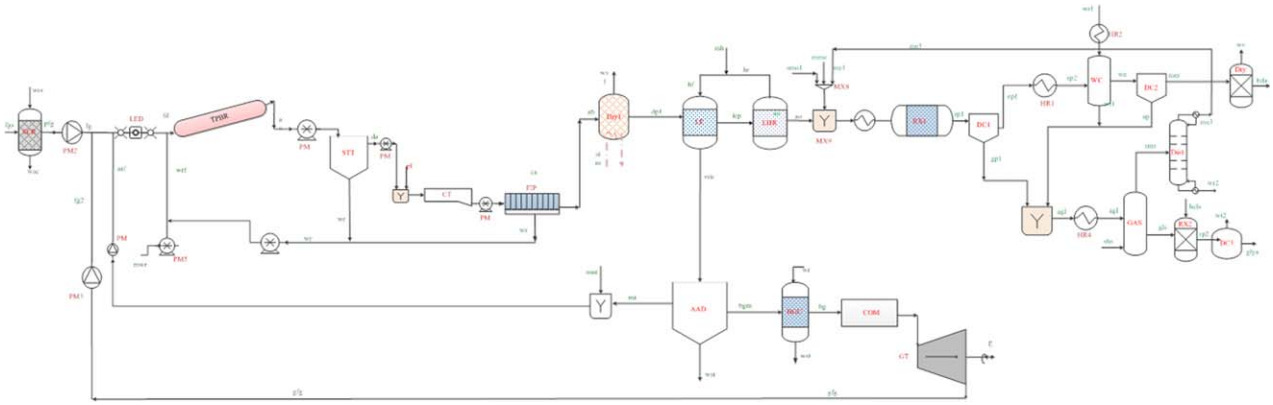

Figure 13. Pareto point B optimal process design includes carbon capture, gas transportation, tubular photobioreactor, filter press dewatering, lipid extraction and sodium methoxide-catalyzed transesterification conversion pathways.

[Color figure can be viewed in the online issue, which is available at wileyonlinelibrary.com.]

biorefinary. In this design, the total CO_2 emissions from the power plant are captured and sequestered; hence, there is no direct emission contribution from the power plant flue gas. Moreover, hydroprocessing produces green diesel which can be used directly by existing infrastructure and automobile engines in greater proportions than ordinary biodiesel. This gives it an advantage in the market over the biodiesel.

Point B**:** As shown in Figure 13, in this design, the processing units are the same as the maximum NPV design except the algal oil upgrading. In this design, the total CO_2 emissions from the power plant are captured and sequestered. As the environmental impact epsilon value becomes lower, the biodiesel production via sodium methoxide transesterification of algal oil becomes more economical. This is due to the fact that the investment cost of this technology is much lower than that of the hydroprocessing and its operational cost is the lowest among the transesterification technology alternatives.

Point C: As shown in Figure 14, in this design, the cap on environmental impact is decreased hence the diesel production decreased. At the trade-off design C, the processing units in each section are similar to those for Point B. As shown in Figure 14, their main difference is that in the current Pareto optimal design, the BPBR, and the flotation dewatering units are selected. The Pareto points below this design have the same configuration. In this design, 16.7% of the CO_2 emissions from the power plants are captured and sequestered. Flue gas (83.3%) from the power plant is vented and hence direct emission contribution from the power plant flue gas is significant. Under industrial biofuel production at this time, given our data, it seems unlikely that the bubble column will be able to scale appropriately.

Table 1 shows the computational times and the objective function values for the four Pareto points by solving with the proposed two-stage algorithm and the commercial global optimization solver BARON 11. As we can see from the table, in terms of the objective function values, the proposed algorithm and the global optimizer BARON gives similar solutions except for Pareto point C. For Pareto point C, the solution from BARON gives a better objective function value. However, the computational time of the proposed algorithm is reduced from the global optimizer BARON on average by a factor of 21.5 for each Pareto point.

Economic analysis

As shown in Figure 15, the investment cost is a major part of the total expenditure for all Pareto points, but for the maximum NPV design that corresponds to the high biofuel

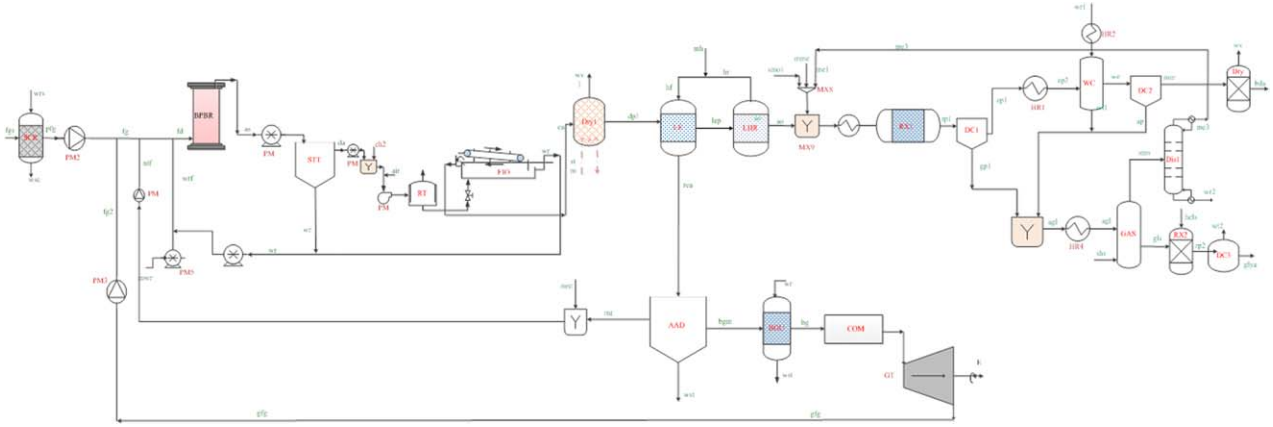

Figure 14. Pareto points C & D optimal process designs include carbon capture, gas transportation, bubble column photobioreactor, flotation dewatering, lipid extraction and sodium methoxide-catalyzed transesterification conversion pathway.

[Color figure can be viewed in the online issue, which is available at wileyonlinelibrary.com.]

Table 1. Solution Comparison between the Two-Stage Solution Algorithm and BARON 11 for the Four Pareto Points

	GWP ($ktonCO_{2\text{-}eq}$/year)		NPV ($MM)		CPU (s)	
	BARON 11	Two-Stage	BARON 11	Two-Stage	BARON 11	Two-Stage
A	5121.93	5121.93	623.48	623.48	5.96	0.31
B	4624.16	4624.16	540.5	540.5	6.47	0.22
C	3852.42	3852.42	−18.66	−53.27	11.78	0.36
D	3610.11	3611.02	−60.14	−59.85	27.3	4.61

production points A and B, the investment cost is mostly dominated by carbon capture that includes the scrubber, pumping station, gas transportation, and artificial lighting cost. The high carbon capture investment cost is followed by the investment cost of the algae growth. The investment costs of carbon capture and algae growth at point A are $305 and $260 million, respectively, making up 70% of the total investment cost of the entire system. Point B has less investment cost in algal oil upgrading. This is because of the low investment cost of the sodium methoxide transesterification pathway compared to the hydroprocessing pathway. At the lower GWP points, the costs are distributed more evenly.

Figure 16 shows the annual operating cost distribution among the processing sections of the selected Pareto points. The largest contribution is from the operating cost of dewatering (46% for point A) followed by the lipid extraction and power generation section (37% for point A), and the algae growth sections. High operating costs arise because of the power and heat consumption in dewatering, high-power consumption of the lipid extraction and biogas upgrading, and the high-power consumption by the algae culture for mixing and degassing of the accumulated gases that can hinder the algae growth.

As shown in Figure 17, the power consumption differs from section to section and from Pareto point to point. Dewatering is the main power consuming section, which consumes between 50 and 70% of total power. This consumption led to a high-operating cost of dewatering shown in Figure 16. It includes the pumping power of algae slurry, power consumption pumping the recycle and makeup water, the pumping power of dilute and concentrated algae, and power consumption by the selected dewatering technology. Depending on the production capacity, dewatering is followed by algae growth for high-production capacity and lipid extraction for lower capacity. The main reason for high-power consumption of the lipid extraction section is the biogas upgrading. The biogas upgrading uses pressurized water to separate the CO_2 from the methane mixture of the biogas. The productivity of the TPBR is the highest among the algae growth PBRs. However, the unit power consumption per volume of the algae growth culture of the TPBR is the highest compared to the FPBR, BPBR, and OP. For Pareto points A and B, the use of the TPBR for algae growth is due to less volume of algae growth culture requirement for high-production capacity relative to the other PBRs. However, as the biofuel production decreases, because of the lower unit power consumption, the BPBR is preferred to the TPBR from the environmental impact perspective.

Environmental impact analysis

Figure 18 shows the contributions to the total GWP from the direct emissions and the GWP from heat and power consumption of the algae-based hydrocarbon biorefineries. The sources of the direct emissions include the flue gas vent from the power plant whenever algae growth capacity is lowered, the unreacted CO_2 emissions during the photobioreactor degassing, and the GHG emissions from the anaerobic digestion. At point D, direct emissions are 99.9% of the total GWP but at point A, they are only 55%. As we move from the minimum GWP design to the maximum NPV design, the biofuel production increases and hence the direct emissions from flue gas venting decreases by 790 $ktonCO_{2\text{-}eq}$ per year. However, because of the high-production rate, the heat and power consumption of each section increase, leading to an increase in the overall GWP contribution.

Figure 19 presents the distribution of the GWP contributions among the algae-based hydrocarbon biorefinery subsections. At higher biofuel production, such as at Pareto points A and B, the contribution from carbon capture and transportation section becomes negligible because no flue gas is vented. Algae growth and dewatering sections are the dominant sources of emissions and environmental impact. The direct emissions from the gas turbine and algal oil upgrading

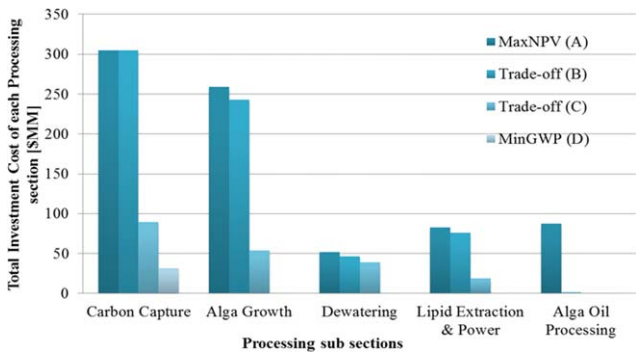

Figure 15. Investment cost distribution among the processing sections of the superstructure.

[Color figure can be viewed in the online issue, which is available at wileyonlinelibrary.com.]

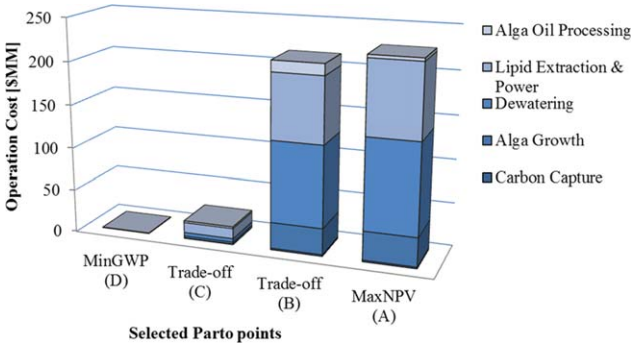

Figure 16. Annual operating cost distribution among the processing sections for the selected Pareto points.

[Color figure can be viewed in the online issue, which is available at wileyonlinelibrary.com.]

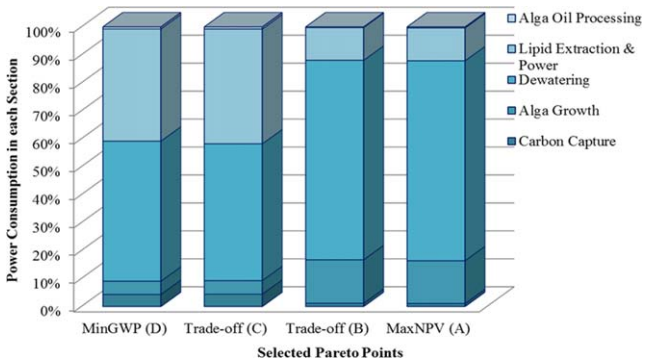

Figure 17. Power consumption distribution among the processing sections of the superstructure.

[Color figure can be viewed in the online issue, which is available at wileyonlinelibrary.com.]

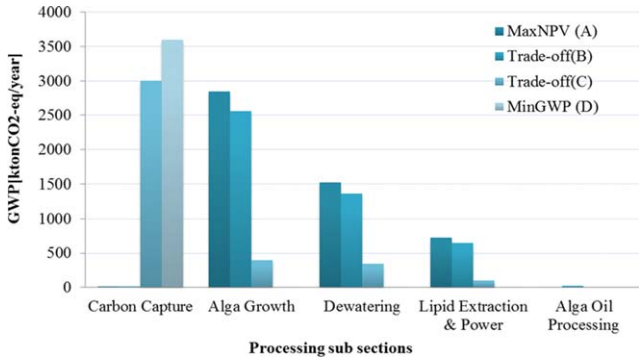

Figure 19. The distribution of GWP contribution among the processing subsections for the selected Pareto points.

[Color figure can be viewed in the online issue, which is available at wileyonlinelibrary.com.]

are recycled back to the algae growth to increase production. At the current level of the technology, more passive systems cannot fill the need for high-level production, but filter press and TPBRs can be scaled easily.

The total project investment cost includes the total equipment purchase cost, engineering, construction, legal and contractor's fee, project contingency, land cost, and working capital cost. The contribution of each cost for the maximum NPV design is given in Figure 20. The investment cost is dominated by the equipment purchase cost of about 42%, but the combined fees for engineering, legal, and contractors represent 24% of the total investment and working capital, such as the machinery together with the project contingency safety factor, represents another 29% of the total expenditure.

Figure 21 shows the annualized total cost and its distribution between annualized investment cost and annual operational cost. As shown in the figure, an investment cost is significant for such complex processing systems. However, as the production increases, the relative significance of investment costs decreases. In the figure, one can see that the maximum production points, A and B, are dominated by operations costs associated with production. In these cases, investment cost is kept to roughly 33% of total annual expenditure while points C and D have much higher investment cost contribution up to 80%.

Sensitivity analysis

Figure 22 shows the Pareto curves at different biofuel prices of the algae-based hydrocarbon biorefinery. The profitability of algae-based biofuels is a strong function of the price of diesel. The current diesel prices limit the design choices for downstream processing, but the model can predict profitability under various price conditions. The trade-offs between technologies are the same and occur at the same points, but the relative economic potential diverges quickly depending on the price of the biofuel and the production capacity. Not only do the technologies get more profitable with more expensive diesel prices, but there also develops a wider spread between technologies making the selection of algal oil biorefinery process alternatives more crucial. Alternative solutions arise as the price of diesel gets higher. If the price of diesel gets all the way to \$10/gal, the sodium methoxide-catalyzed transesterification is still economically the viable technology option across the large portion of the Pareto points.

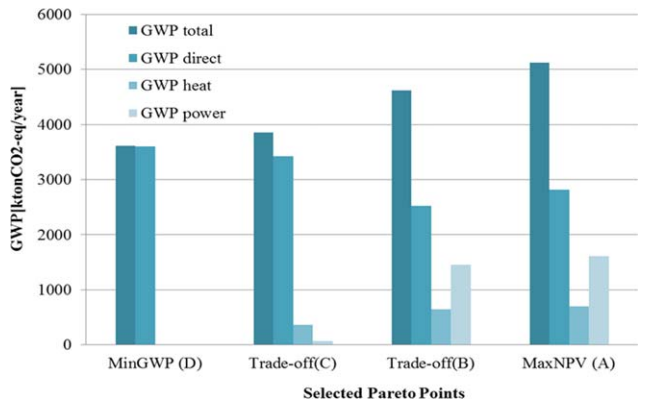

Figure 18. The distribution of GWP contributions among the direct emissions, heat- and power-related emissions for the selected Pareto points.

[Color figure can be viewed in the online issue, which is available at wileyonlinelibrary.com.]

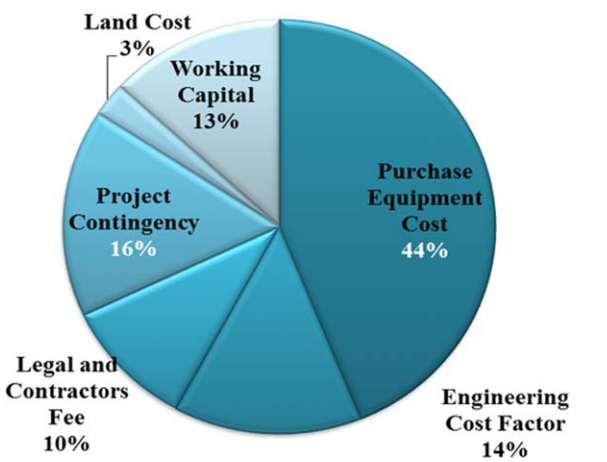

Figure 20. Total project investment cost distribution for maximum NPV design (point A).

[Color figure can be viewed in the online issue, which is available at wileyonlinelibrary.com.]

The increased NPV is entirely due to the fact that GWP rises in lockstep with production within the range of one technology. Figure 16 shows that the lowest ends of production remain tied to the GWP from direct emissions from the power plant, up to 3600kton/year of carbon dioxide. The slope of the Pareto curve changes depending on the value of diesel. The more revenue is generated through increased productivity, the more quickly NPV rises. The changes in technology are really just superficial because dewatering and algae growth are the main costs in the system. Technology advances in these areas will have the greatest effect on NPV.

Conclusions

In this article, we proposed a multiobjective MINLP model for the optimal design and synthesis of algae-based hydrocarbon biorefinery that encompass carbon capture, algae growth, harvesting, lipid extraction, anaerobic digestion, power generation, and algal oil biorefinery under economic and environmental criteria. The economic objective is measured by the NPV, and the measure of environmental impacts is GWP metric. We propose a process superstructure considering multiple technological alternatives that include the selection between direct use of flue gas or pure CO_2 technologies, among OP, tubular, bubble column, and FPBR technologies, among floatation, filtration, and centrifuging dewatering technologies, and finally the algal biorefinery technologies that include sodium methoxide, heterogeneous, and enzyme-catalyzed transesterification, supercritical methanol transesterification and hydroprocessing. Based on the superstructure, we developed a bicriteria MINLP model and solved following a two-stage heuristic solution algorithm for the simultaneous maximization the NPV and minimization the GWP, subject to the mass balance, energy balances, and economic analysis and life cycle environmental impact constraints.

The bicriteria problem is solved with the ε-constraint method. The resulting Pareto-optimal curve reveals the trade-off between the economic and environmental performances. The optimal solution reveals that the combination of the direct use of flue gas, TPBR algae growth technology, filtration dewatering technology, and hydroprocessing technology have better economic performance. However, for the best environmental impact performance, the hydroprocessing technology is replaced by the sodium methoxide-catalyzed transesterification. In the maximum NPV design, the unit production cost of the green diesel is \$6.33/gal while the corresponding NPV of \$623.8 MM and GWP of 5122 ktonCO$_{2\text{-eq}}$ per year.

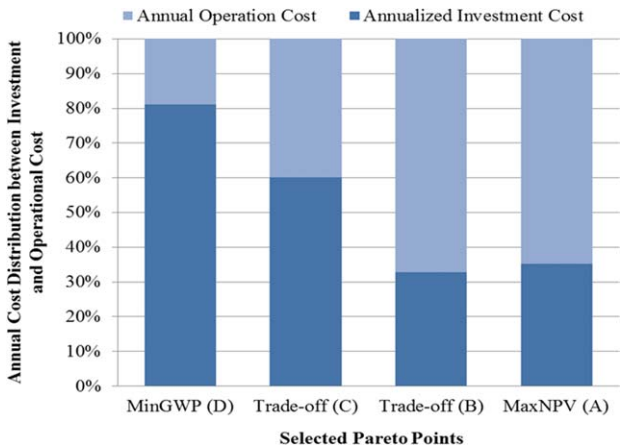

Figure 21. Annual operation and annualized investment cost of the selected Pareto points.

[Color figure can be viewed in the online issue, which is available at wileyonlinelibrary.com.]

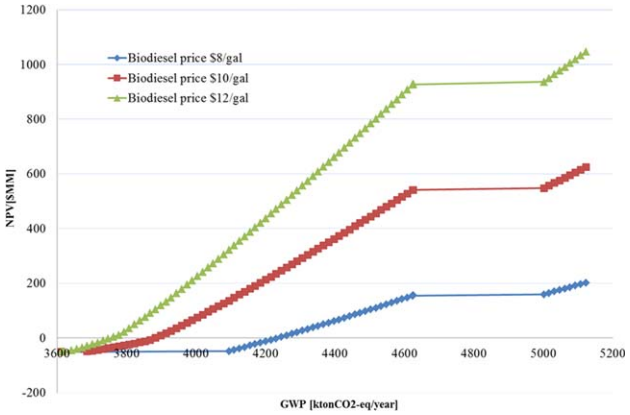

Figure 22. Pareto curves at different biodiesel price of the algal biorefinery system.

[Color figure can be viewed in the online issue, which is available at wileyonlinelibrary.com.]

A possible future extension is expanding the superstructure to include advanced and energy efficient technologies, such as the dewatering, algae growth PBRs, and biogas upgrading technologies. Another future research path is combining energy integration modeling and the superstructure optimization.

Acknowledgments

The authors are grateful to Ms. Victoria Perez (Northwestern University) for the discussion and comments. The authors gratefully acknowledge the financial support from the Initiative for Sustainability and Energy at Northwestern University (ISEN).

Notation

Set

J_{ccs} = set of species involved in carbon capture and algae growth
J_{dw} = set of species involved in dewatering section
J_{lep} = set of species involved in lipid extraction, anaerobic digestion
J_{bdpt} = set of species involved in algal biorefinery technology *bdpt*.
agt = algae growth technologies
dwt = dewatering technologies
bdpt = algal biorefinery technologies
abs = flue gas and absorption separation modeling

Variables

AGP = annual gross profit, \$MM
aoc = the total annual operating cost, \$MM
APAT = annual profit after tax, \$MM
apic = the total project investment cost, \$MM
apec = the total annualized equipment purchase cost, \$MM
D = pipe diameter, m
ecc_l = purchase cost of unit l, \$MM
eic_l = the purchase cost of equipment l at year of interest, \$MM
fixc = fixed O&M cost, \$MM
gwp = global warming potential, ktonCO$_{2\text{-eq}}$/year
INCV = total volumetric incentive, \$MM

INCC = total investment incentive, $MM
lp = length of transportation pipe, km
$m^l_{s,k,j}$ = mass flow rate of species j of stream s in technology k and equipment l
$\bar{m}^l_{s,k}$ = total mass flow rate of stream s of technology k and equipment l
NPV = net present value, $MM
opc_j = operating cost contribution from consumption of j, $MM
pd = discharge pressure, Mpa
prc = cost of power cost, $MM
ps = suction pressure, Mpa
pr_l = power consumption of unit l, MW
Q = volumetric flow rate, m^3/h
qhc = cost of heat cost, $MM
Rev = revenue, $MM
tac = total annual cost, $MM
$v_{R,agt}$ = volume of algae growth technology agt
y_{agt} = binary variable to model selection of algae growth technology
y_{dwt} = binary variable to model selection of dewatering technology
y_{bdpt} = binary variable to model selection of alga-oil processing technology
y_{abs} = binary variable to model selection of direct flue gas or pure CO_2
$V_{bg,wr}$ = volume of water required for biogas upgrading

Parameters

AFR_{gt} = air fuel ratio for gas turbine combustion
CEPCI = Chemical Engineering Plant Cost Index
CMGAL = conversion factor from cubic meters to gallons
$CONC^s_j$ = concentration of species j in solution, s
CRF = capital recovery factor
ECC^l_b = base case purchase cost of equipment l, $MM
E_{air} = fraction of excess air
GMG = conversion from gallons to millions of gallons
HD = total hours per day, h
INCM = maximum allowable investment incentive, $MM
INCP = percentage of investment incentive
IR = interest rate
KGKT = conversion factor from kilograms in a kilo tone
K_{ENG} = engineering cost factor
K_{LCF} = legal and contractors fee factor
K_{LND} = cost factor of land
K_{OM} = O& M cost as percentage of the total equipment purchase cost
K_{PCC} = project contingency factor
K_{WCP} = working capital cost factor
Mw_j = molecular weight of species j
NHD = nolight hours per day, h
PER^l_s = percentage of stream s with respect to the fed to equipment l
ppm^{fgs}_j = fraction of SO_x and NO_x in the feed flue gas stream
$PRICE_j$ = unit price of j
$P_{R,agt}$ = productivity of algae growth technology agt
$RAT_{A/S}$ = air to solid ratio fraction
RAT^v_{bgwr} = the volumetric ratio of biogas to water used for upgrading
$R^l_{k,j}$ = conversion of species j in unit l of technology k
R_{tax} = income tax
sf = sizing factor
SH = total seconds per hour
$S^l_{s,j}$ = split fraction of species j in separation unit l
$SC_{agt,j}$ = stoichiometric consumption of species j in algae growth technology agt
$STC_{i,j}$ = stoichiometric coefficient of species j when reacting species i
T_{dp} = the depreciation time of the project, years
T_{op} = annual operating hours of the biorefinery, h/year
T_{ls} = lifespan of the hydrocarbon biorefinery, years
$UCC_{abs,agt}$ = unit CO_2 consumption depending on the type of gas feed abs and algae growth technology agt.
UB = upper bound of the product stream from dewatering
UNC^{ag}_j = unit nutrient j consumption per grams of algae harvested
UWC^{ag}_{agt} = unit mass of water consumed in algae growth technology agt
$WF^l_{s,k,j}$ = weight fraction of species j in stream s of technology k and unit l
α^{hrx}_j = product distribution of hydrogenation product species j
β^{scr}_{wrs} = scrubber liquid to gas ratio
$\beta^{lea}_{hex,loss}$ = fraction of hexane lose with the residue
β^{bg}_{met} = fraction of methane recovery in the biogas upgrading
β^{nut}_j = fraction of nutrient j recovery
β^{le}_{hex} = hexane ratio required for lipid extraction
β^{lep}_{lip} = lipid extraction efficiency
β_{mea} = makeup solvent in ton per ton of CO_2 separated in MEA
β^{recy}_{hex} = hexane recycle ratio from the hexane lipid recovery
β^{aad}_j = ratio of anaerobic digester product j with respect to the suspended solids feed
$\beta^{mef}_{bdpt,j}$ = methanol and t-butanol molar feed ratio with respect to the triglyceride feed for technology bdpt
Φ_b = the damage factor that accounts for the GWP associated with chemical species b

Subscripts/superscript

al = dry algae species
ao = algal oil/lipids
ap = aqueous phase stream
bd = biodiesel
ca = concentrated algae stream from the dewatering units
cgf = centrifuge feed stream; outlet stream from the mixer
ch = polymer additive stream that joins da and flows into the conditioning tank
cog = coagulant stream to the mixer
da = dilute algae stream
dp1 = partially dried algae exits
ep = methyl ester-rich stream
gd = green diesel
gp = gasoline-rich stream
flf = flotation feed; outlet stream from pressure retention tank
fpf = filter Press feed, outlet stream of conditioning tank
HCl = hydrochloric acid solution
me = methanol
mer = methyl ester-rich stream
mme = makeup methanol
mx = discharge from the mixer that has not been aerated
pf = polymer stream
ret = pressurized mixed stream from the aeration unit
rp = reactor product
smo = sodium methoxide
sms = saturated methanol-rich stream
we = washed methyl ester stream
wr = water species
wv = water vapor

Literature Cited

1. Ferrel J, Sarisky-Reed V. National algal biofuels technology roadmap. In: *Energy Efficiency & Renewable Energy*. College Park, MD: US Department of Energy, 2010.
2. Chen Y, Adams TA II, Barton PI. Optimal design and operation of flexible energy polygeneration systems. *Ind Eng Chem Res.* 2011;50(8):4553–4566.
3. Baliban RC, Elia JA, Misener R, Floudas CA. Global optimization of a MINLP process synthesis model for thermochemical based conversion of hybrid coal, biomass, and natural gas to liquid fuels. *Comput Chem Eng.* 2012;42(0):64–86.
4. Martin M, Grossmann IE. Energy optimization of bioethanol production via gasification of switchgrass. *AIChE J*. 2011;57(12):3408–3428.
5. Grossmann IE, Martin M. Energy and water optimization in biofuel plants. *Chin J Chem Eng*. 2010;18(6):914–922.
6. Liu P, Gerogiorgis DI, Pistikopoulos EN. Modeling and optimization of polygeneration energy systems. *Catal Today*. 2007;127(1–4):347–359.
7. Liu P, Georgiadis MC, Pistikopoulos EN. Advances in energy systems engineering. *Ind Eng Chem Res*. 2011;50(9):4915–4926.
8. Wang B, Gebreslassie BH, You F. Sustainable design and synthesis of hydrocarbon biorefinery via gasification pathway: integrated life cycle assessment and technoeconomic analysis with multiobjective superstructure optimization. *Comput Chem Eng*. 2013;52:55–76.
9. Gebreslassie BH, Slivinsky M, Wang B, You F. Life cycle optimization for sustainable design and operations of hydrocarbon biorefinery

via fast pyrolysis, hydroprocessing and hydrocracking. *Comput Chem Eng*. 2013;50:71–91.
10. Martin M, Grossmann IE. Simultaneous optimization and heat integration for biodiesel production from cooking oil and algae. *Ind Eng Chem Res*. 2012;51(23):7998–8014.
11. West AH, Posarac D, Ellis N. Assessment of four biodiesel production processes using HYSYS.Plant. *Bioresour Technol*. 2008;99:6587–6601.
12. Gutierrez LF, Sanchez OJ, Cardona CA. Process integration possibilities for biodiesel production from palm oil using ethanol obtained from lignocellulosic residues of oil palm industry. *Bioresour Technol*. 2009;100(3):1227–1237.
13. Severson K, Martín M, Grossmann IE. Optimal integration for biodiesel production using bioethanol. *AIChE J*. 2013;50(3):834–844.
14. Davis R, Aden A, Pienkos PT. Techno-economic analysis of autotrophic microalgae for fuel production. *Appl Energy*. 2011;88(10): 3524–3531.
15. Davis R. *Techno-Economic Analysis of Microalgae-Derived Biofuel Production*. Golden, CO: US Department of Energy, National Renewable Energy Laboratory, 2009.
16. Pokoo-Aikins G, Nadim A, El-Halwagi MM, Mahalec V. Design and analysis of biodiesel production from algae grown through carbon sequestration. *Clean Technol Envir*. 2010;12(3):239–254.
17. Cano-Ruiz JA, McRae GJ. Environmentally conscious chemical process design. *Annu Rev Energ Environ* 1998 1998;23:499–536.
18. IRAM-ISO-14040. *Environmental management-life cycle assessment-principles and frame work*. International Standard: ISO, Geneva, Switzerland, 2006.
19. Chapel DG, Mariz CL, Ernst J. *Recovery of CO_2 from Flue Gases: Commercial Trends*. In: Canadian Society of Chemical Engineers Annual Meeting, Saskatoon, Saskatchewan, 1999.
20. Fisher KS, Beitler C, Rueter C, Searcy K. *Integrating MEA Regeneration with CO_2 Compression and Peaking to Reduce CO_2 Capture costs*. Buda, TX: Trimeric Corporation, University of Texas at Austin, 2005.
21. Miron AS, Camacho FG, Gomez AC, Grima EM, Chisti Y. Bubble-column and airlift photobioreactors for algal culture. *AIChE J*. 2000;46(9):1872–1887.
22. Sánchez Mirón A, Cerón García MC, García Camacho F, Molina Grima E, Chisti Y. Mixing in bubble column and airlift reactors. *Chem Eng Res Des*. 2004;82(10):1367–1374.
23. Sierra E, Acien FG, Fernandez JM, Garcia JL, Gonzalez C, Molina E. Characterization of a flat plate photobioreactor for the production of microalgae. *Chem Eng J*. 2008;138(1–3):136–147.
24. Acién Fernández FG, Fernández Sevilla JM, Sánchez Pérez JA, Molina Grima E, Chisti Y. Airlift-driven external-loop tubular photobioreactors for outdoor production of microalgae: assessment of design and performance. *Chem Eng Sci*. 2001;56(8):2721–2732.
25. Molina E, Fernández J, Acién FG, Chisti Y. Tubular photobioreactor design for algal cultures. *J Biotechnol*. 2001;92(2):113–131.
26. Stephenson AL, Kazamia E, Dennis JS, Howe CJ, Scott SA, Smith AG. Life-cycle assessment of potential algal biodiesel production in the United Kingdom: a comparison of raceways and air-lift tubular bioreactors. *Energy Fuels*. 2010;24:4082–4077.
27. Chisti Y. Biodiesel from microalgae. *Biotechnol Adv*. 2007;25(3):294–306.
28. Cheng-Wu Z, Zmora O, Kopel R, Richmond A. An industrial-size flat plate glass reactor for mass production of *Nannochloropsis* sp. (Eustigmatophyceae). *Aquaculture*. 2001;195(1–2):35–49.
29. Chen C-Y, Yeh K-L, Aisyah R, Lee D-J, Chang J-S. Cultivation, photobioreactor design and harvesting of microalgae for biodiesel production: a critical review. *Bioresour Technol*. 2011;102(1):71–81.
30. Zlender B, Kravanja S. Cost optimization of the underground gas storage. *Eng Struct*. 2011;33(9):2554–2562.
31. Sinnott RK. *Coulson & Richardson's Chemical Engineering, Vol 6: Chemical Engineering Design*. MA: Elsevier Butterworth-Heinemann, 2005.
32. Sheehan J, Dunahay T, Benemann J, Roessler P. A look back at the US Department of Energy's Aquatic Species Program—biodiesel from Algae. Golden, CO: National Renewable Energy Laboratory, 1998.
33. Lundquist TJ, Woertz IC, Quinn NWT, Benemann JR. *A Realistic Technology and Engineering Assessment of Algae Biofuel Production*. Berkeley: Energy Biosciences Institute, University of California, 2010.
34. Shelef GS, Sukenik A, Green M. *Microalgae Harvesting and Processing: A Literature Review*. Golden, CO: Solar Energy Research Institute SERI, 1984.
35. Wang LK, Shammas NK, Selke WA, Aulenbach DB. *Handbook of Environmental Engineering, Vol 6: Biosolids Treatment Processes*, Totawa, NJ: Humana Press Inc., 2007.
36. Ehimen EA, Sun ZF, Carrington CG, Birch EJ, Eaton-Rye JJ. Anaerobic digestion of microalgae residues resulting from the biodiesel production process. *Appl Energ*. 2011;88:3454–3463.
37. Collet P, Helias A, Lardon L, Ras M, Goy R-A, Steyer J-P. Life-cycle assessment of microalgae culture coupled to biogas production. *Bioresour Technol*. 2011;1002(1):207–214.
38. Apostolakou AA, Kookos IK, Marazioti C, Angelopoulos KC. Techno-economic analysis of a biodiesel production process from vegetable oils. *Fuel Process Technol*. 2009;90(7–8):1023–1031.
39. Sakai T, Kawashima A, Koshikawa T. Economic assessment of batch biodiesel production processes using homogeneous and heterogeneous alkali catalysts. *Bioresour Technol*. 2009;100(13):3268–3276.
40. D'Cruz A, Kulkarni MG, Meher LC, Dalai AK. Synthesis of biodiesel from canola oil using heterogeneous base catalyst. *J Am Oil Chem Soc*. 2007;84(10):937–943.
41. Sotoft LF, Rong B-G, Christensen KV, Norddahl B. Process simulation and economical evaluation of enzymatic biodiesel production plant. *Bioresour Technol*. 2010;101(14):5266–5274.
42. Sawangkeaw R, Teeravitud S, Piumsomboon P, Ngamprasertsith S. Biofuel production from crude palm oil with supercritical alcohols: comparative LCA studies. *Bioresour Technol*. 2012;120:6–12.
43. Kalnes T, Marker T, Shonnard DR. Green diesel: a second generation biofuel. Int J Chem React Eng. 2007;5:1–11. DOI: 10.2202/1542-6580.1554.
44. Huo H, Wang M, Bloyd C, Putsche V. *Life-Cycle Assessment of Energy and Greenhouse Gas Effects of Soybean-Derived Biodiesel and Renewable Fuels*. Argonne National Laboratory: US Department of Energy, Oak Ridge, TN, 2008.
45. Tapasvi D, Wiesenborn D, Gustafson C. Process model for biodiesel production from various feedstocks. *Trans ASAE*. 2005;48(6):2215–2221.
46. Sheehan J, Camobreco V, Duffield J, Graboski M, Shapouri H. *An Overview of Biodiesel and Petroleum Diesel Life Cycles*. Golden, CO: US Department of Agriculture and US Department of Energy;1998.
47. Kasteren JMN, Nisworo AP. A process model to estimate the cost of industrial scale biodiesel production from waste cooking oil by supercritical transesterification. *Resour Conserv Recy*. 2007;50(4):442–458.
48. D'Cruz A, Kulkarni MG, Meher LC, Dalai AK. Synthesis of Biodiesel from Canola oil using heterogeneous base catalyst. *J Am Oil Chem Soc*. 2007;84:937–943.
49. Huang Y, Zheng H, Yunjun Y. Optimization of lipase-catalyzed transesterification of lard for biodiesel production using response surface methodology. *Appl Biochem Biotechnol*. 2010;160:504–515.
50. Azapagic A, Clift R. Life cycle assessment and multiobjective optimisation. *J Clean Prod*. 1999;7(2):135–143.
51. Azapagic A, Clift R. The application of life cycle assessment to process optimisation. *Comput Chem Eng*. 1999;23(10):1509–1526.
52. Azapagic A. Life cycle assessment and its application to process selection, design and optimisation. *Chem Eng J*. 1999;73(1):1–21.
53. Solomon S, Qin D, Manning M, Chen M, Marquis Z, Averyt M, Tignor KB, Miller. HL. *Contribution of Working Group I to the Fourth Assessment Report of the Intergovernmental Panel on Climate Change*. Technical Report, UK and New York: Cambridge University Press, 2007.
54. Ecoinvent Center. A Competence Centre of ETH, PSI, Empa and ART. *ecoinvent data* Swiss Centre for Life Cycle Inventories, ETH Zurich, v2.12009.
55. PE International. GaBi: Software and database contents for life cycle, engineering. In: http://www.gabi-software.com/america/databases, ed. PE International: Stuttgart, Germany, 2011.
56. GREET. *The greenhouse gases, regulated emissions, and energy use in transportation model*. In: http://greet.es.anl.gov/, ed: Oak Ridge, TN: Argonne National Laboratory, 2012.
57. Gian-Kasper P, Stocker T, Midgley P, Tignor M. In: *IPCC Expert Meeting on the Science of Alternative Metrics,* 2009.
58. CEPCI. Chemical Engineering Plant Cost Index (CEPCI). 2011; available at: www.che.com/pci/.

59. McCoy S. *A Technical and Economic Assessment of Transport and Storage of CO2 in Deep Saline Aquifers for Power Plant Greenhouse Gas Control*. Pittsburgh, PA. 15213: Carnegie Mellon Electricity Industry Center Working Paper; 2005.
60. Federal & State incentives & Laws. Alternative Fuels data center. Available at: www.afdc.energy.gov/afdc/laws/laws/US/tech/325, 2012 (accessed May 2012).
61. You FQ, Tao L, Graziano DJ, Snyder SW. Optimal design of sustainable cellulosic biofuel supply chains: multiobjective optimization coupled with life cycle assessment and input-output analysis. *AIChE J*. 2012;58(4):1157–1180.
62. Gebreslassie BH, Yao Y, You FQ. Design under uncertainty of hydrocarbon biorefinery supply chains: multiobjective stochastic programming models, decomposition algorithm and a comparison between cvar and downside risk. *AIChE J*. 2012;58(07):2155–2179.
63. You FQ, Wang B. Life cycle optimization of biomass-to-liquid supply chains with distributed-centralized processing networks. *Ind Eng Chem Res*. 2011;50(17):10102–10127.
64. Tawarmalani M, Sahinidis NV. A polyhedral branch-and-cut approach to global optimizatio. *Math Program.* 2005;103(2):225–249.
65. You F, Grossmann IE. Mixed-integer nonlinear programming models and algorithms for large-scale supply chain design with stochastic inventory management. *Ind Eng Chem Res*. 2008;47(20):7802–7817.
66. Padberg M. Approximating separable nonlinear functions via mixed zero-one programs. *Oper Res Lett*. 2000;27(1):1–5.
67. Yue D, You F. Planning and scheduling of flexible process networks under uncertainty with stochastic inventory: MINLP models and algorithm. *AIChE J*. In press. DOI: 10.1002/aic.13924.
68. Ehrgott M. *Multicriteria Optimization*. Berlin, Heidelberg: Springer, 2000.
69. Rosenthal RE. *GAMS—A User's Manual*. Washington, DC: GAMS Development Corp., 2011.

Manuscript received Oct. 12, 2012, and revision received Jan. 3, 2013.